(NASA-TM-X-71997) SENSITIVITY OF GAS FILTER CORRELATION INSTRUMENT TO VARIATIONS IN OPTICAL BALANCE (NASA) 49 p HC $3.75 CSCL 14B

N75-19622

Unclas G3/35 13372

NASA TECHNICAL MEMORANDUM

NASA TM X-71997

COPY NO.

NASA TM X-71997

SENSITIVITY OF GAS FILTER CORRELATION INSTRUMENT TO VARIATIONS IN OPTICAL BALANCE

HARRY D. ORR, III

AND

SHIRLEY A. CAMPBELL
LTV AEROSPACE CORPORATION
HAMPTON, VIRGINIA 23666

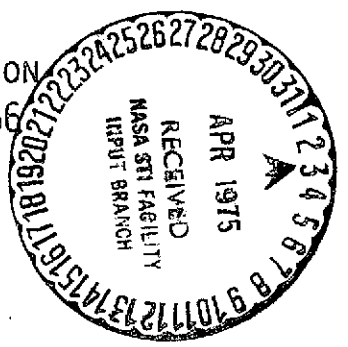

NATIONAL AERONAUTICS AND SPACE ADMINISTRATION
LANGLEY RESEARCH CENTER, HAMPTON, VIRGINIA 23665

1. Report No.	2. Government Accession No.	3. Recipient's Catalog No.
NASA TM X-17797		

4. Title and Subtitle	5. Report Date
Sensitivity of a Gas Filter Correlation Instrument to Variations in Optical Balance	January 28, 1975
	6. Performing Organization Code: 6312
7. Author(s): Harry D. Orr, III and Shirley A. Campbell*	8. Performing Organization Report No.: NASA TM X-17797
	10. Work Unit No.: 642-12-12-01-00
9. Performing Organization Name and Address: National Aeronautics and Space Administration, Langley Research Center, Hampton, Virginia 23665	11. Contract or Grant No.
	13. Type of Report and Period Covered: NASA Technical Memorandum
12. Sponsoring Agency Name and Address	14. Sponsoring Agency Code

15. Supplementary Notes

*LTV Aerospace Corporation

Special technical information, not planned for formal NASA publication

16. Abstract

The sensitivity of a simple Gas Filter Correlation Radiometer (GFCR) to variations in the instrument's optical balance parameter, τ_A, has been studied theoretically.

A computer program was used to simulate the response of the GFCR to changing pollutant levels of CO, SO_2, CH_4, and NH_3 in two model atmospheres. Positive and negative deviations of τ_A of magnitudes 0.01, 0.1, and 1 percent were imposed upon the simulation and the resulting deviations in inferred concentrations were determined.

For the CO, CH_4, and the higher pressure cell of the NH_3 channel, the deviations are less than ± 12 percent for deviations in τ_A of ± 0.1 percent, but increase to significantly higher values for larger deviations. For the lower pressure cell of NH_3 and for SO_2, the deviations in inferred concentration begin to rise sharply between 0.01 and 0.1 percent deviation in τ_A, suggesting that a tighter control on τ_A may be required for these channels.

17. Key Words (Suggested by Author(s)) (STAR category underlined)

Instrumentation and Photography
Infrared Technology
Instrument Standards
Remote Sensing
Computer Simulation
Atmospheric Trace Constituents

18. Distribution Statement

19. Security Classif. (of this report)	20. Security Classif. (of this page)	21. No. of Pages	22. Price*
Unclassified	Unclassified	47	$3.75

*Available from { The National Technical Information Service, Springfield, Virginia 22151 / STIF/NASA Scientific and Technical Information Facility, P.O. Box 33, College Park, MD 20740

SENSITIVITY OF A GAS FILTER CORRELATION INSTRUMENT TO VARIATIONS IN OPTICAL BALANCE

By

Harry D. Orr, III and Shirley A. Campbell

ABSTRACT

The sensitivity of a simple Gas Filter Correlation Radiometer (GFCR) to variations in the instrument's optical balance parameter, τ_A, has been studied theoretically.

A computer program was used to simulate the response of the GFCR to changing pollutant levels of CO, SO_2, CH_4, and NH_3 in two model atmospheres. Positive and negative deviations of τ_A of magnitudes 0.01, 0.1, and 1 percent were imposed upon the simulation and the resulting deviation in inferred pollutant concentration were determined.

For the CO and CH_4 channels, and the higher pressure cell of the NH_3 channel, the deviations are less than ± 12 percent for the deviations in τ_A of ± 0.1 percent, but increase to significantly higher values for larger deviations. For the lower pressure cell of the NH_3 channel and for the SO_2 channel, the deviations in inferred concentration begin to rise sharply between 0.01 and 0.1 percent deviation in τ_A, suggesting that a tighter control on τ_A may be required for this channel.

I. INTRODUCTION

The concept of measuring the total burden or column density of trace gases by nondispersive infrared techniques is currently an area of much interest. One variety of this technique, the gas filter correlation radiometer (GFCR), is being explored for both aircraft and satellite applications to the measurement of pollutant gas concentrations (refs. 1-2). The operation of the instrument depends not only upon the various parameters describing the underlying surface and atmosphere, but also upon those describing the instrument's physical state

-- for example, the temperature, emissivities and reflectivities of various optical components. Moreover, the reliability of the data from such an instrument is strongly affected by the stability of these parameters. This report presents the results of a theoretical study of the sensitivity of the GFCR to one such parameter, the vacuum - cell aperture transmission, τ_A, which is used to mechanically balance the optical paths of the instrument under conditions of no pollutant gas. The role of this aperture is described in the following section. A list of symbols is given in Appendix B.

II. THEORY OF OPERATION OF GFCR

Detailed descriptions of instruments based on the gas filter correlation technique have been presented elsewhere (see, for example, refs. 1-2). In this work, only the basic elements of a prototype instrument will be described. Figure 1 is a schematic diagram of a simple GFCR. Radiation from the earth's surface and intervening atmosphere enter through the front window. One half of the energy is blocked by a chopper blade; the other half is passed through a lens, then through a cell containing a sample of the gas of interest, and is focused onto a detector. One half cycle later, the chopper blocks the energy on the right hand side and passes it on the left hand side, which contains an empty cell and an adjustable aperture. The difference between the two signals can be expressed as a differential radiance, ΔN, proportional to an instrument voltage, ΔV:

$$\Delta V \alpha \Delta N \alpha \int_{\Delta\nu} E(\nu) \left[C(\nu)\, \tau_G - C'(\nu)\, \tau_A\right] d\nu \qquad (1)$$

where $E(\nu)$ is the incident radiation at wavenumber ν, $C(\nu)$, and $C'(\nu)$ are the transfer functions of the optical components of the right and left hand paths, respectively, $\tau_G(\nu)$ is the wavenumber-dependent transmittance of the reference gas, and τ_A is the wavenumber-independent transmittance of the aperture of the vacuum cell. The filter accepts radiation in the bandpass $\Delta\nu$. The signals also may be combined to give an integral radiometer measurement:

$$V \alpha N \alpha \int_{\Delta\nu} E(\nu) \left[C(\nu)\, \tau_G(\nu) + C'(\nu)\, \tau_A\right] d\nu \qquad (2)$$

When none of the gas of interest is present outside the instrument, the dependence of E on ν is very weakly correlated with the dependence of τ_G on ν. In practice this condition is achieved by alternately placing a hot and then a cold blackbody at the entrance window. The change in ΔV is then minimized by mechanically adjusting the aperture transmission, τ_A. This procedure is commonly referred to as "balancing" the instrument. When the gas of interest is present outside the instrument, in the atmosphere or in a calibration cell, the dependence of E on ν is altered by absorption and emission at the same wavenumbers as are active in the instrument gas cell. This correlation produces an imbalance in the signal strengths between the two optical paths and causes the output signal to deviate from its "balance" value. At the same time, the integral radiance signal, V, is strongly related to the brightness temperature of the background surface.

III. DATA REDUCTION PROCEDURE

Since it is not currently possible to simulate accurately the infrared activity of the earth's atmosphere in the laboratory, theoretical techniques must be used to relate the voltage output of the instrument to the gas burden measured. The primary tool used in this effort is a line-by-line radiative transfer program "POLAYER" (ref. 3). For the purpose of this program, the background surface (either the earth or a laboratory source) is described by a temperature and emissivity; the intervening atmosphere is specified in the form of one or more layers with a thickness, pressure, temperature, and concentration of gases. The instrument is described in terms of the temperature and spectral transmittances of the various components of each of its optical paths. Then, the radiation reaching the detector along each of the optical paths is computed by integrating over $\Delta\nu$ the surface radiation, as modified by any absorbing spectral lines in each layer, plus contributions by any emitting spectral lines in each layer. This procedure is employed in three stages. First, the theoretical value of τ_A is computed which will produce equal values of ΔN for the known laboratory sources with no gases between the sources and the instrument. Next, using this value of τ_A, a description corresponding to the calibration cell used with the instrument is inserted into the program. The results of this calculation establish a relation between the voltages measured by the instrument and the corresponding values of

radiance. The real atmosphere with its inherent non-homogeneity, cannot be simulated by such cells; thus in the third stage a description of the real atmosphere, to whatever accuracy it is known at the time of measurement, is inserted. The response of the instrument to the radiances associated with a range of potential concentrations of the gas of interest is computed. Figures 2 - 5 show the responses of the instrument to the standard atmosphere used in this study. To infer the actual concentration, the voltage calibration from stage two is used to convert the instrument output to radiance units (e.g., watts/cm^2 sr); then the corresponding gas concentration is found by interpolation on the response curve generated in stage three.

IV. METHODOLOGY

In the present work, the sensitivity of the GFCR was studied in four spectral regions, corresponding to wavelengths that might be used in measurement of carbon monoxide (CO), methane (CH_4), sulfur dioxide (SO_2), and ammonia (NH_3), for two pressures of the instrument gas cell (one in the case of SO_2). The details of these conditions are given in table 1.

To use the POLAYER program, two atmospheric models were constructed. In each model, the region from the surface to 22 km was divided into five layers. The layers were chosen so that each contains an approximately equal column density of gas (molecules). The details of the layers are given in table 2.

Model 1 is based on the U.S. Standard Atmosphere, 1962 (ref. 4). The mean temperature of each of the five layers was determined by weighting the U.S. Standard temperatures with the corresponding density values. The vertical distribution of water vapor was taken as that of the Gutnick Model (ref. 5).

Model 2 is based on the U.S. Standard Atmosphere Supplements, 1966, 45°N. latitude for July (ref. 6). The water vapor distribution was taken from the midlatitude summer atmospheric profile of AFCRL Optical Properties of the Atmosphere (ref. 7).

For both models, a surface emissivity of .98 was used; a nighttime measurement was assumed, hence no solar contribution was included. For Model 1, a ground temperature of 288K was used. While the concentrations of all other species

were held constant, the concentration of the pollutant gas of interest, uniformly distributed, was varied in ten steps below and above its nominal or background level. For Model 2, a ground temperature of 296K was used. The details of the distributions are given in table 2.

For each instrument channel and atmospheric model combination, seven response function curves were computed, one corresponding to the standard or correct value of τ_A and six other curves corresponding to variations in τ_A of $\pm 1\%$, $\pm .1\%$, and $\pm .01\%$ from its standard value.

To simulate measurements, four values of ΔN were then selected, and the corresponding values of pollutant concentration were determined by interpolation on each of the seven curves. For each of the four ΔN values, the differences between the indicated concentration in the standard case and the concentrations found in the six varied cases were calculated.

V. RESULTS

The results of the procedure described above are plotted in figures 6 - 13 and tabulated in Appendix A. Each figure, corresponding to a particular species, cell condition, and atmospheric model, shows the percent deviation of the inferred concentration as a function of the percent deviation of τ_A from its standard value.

For all cases, the relative behaviors of the deviations are similar. As τ_A is decreased from its standard values, the percent deviations in inferred concentration become increasingly negative; as τ_A is increased, the deviations become positive. The rate of change of the deviation also appears to increase with deviations in τ_A. For CO, CH_4, and cell 1 of the NH_3 channel magnitudes of deviations of inferred concentrations undergo a sharp rise as the deviations in τ_A exceed $\pm 0.1\%$. For cell 2 of NH_3 and SO_2 the rise commences at even lower deviations in τ_A.

The deviations for CO, CH_4, and NH_3 for a given atmospheric model are lower for the cell with the higher concentration. The reason for this behavior can be seen in figures 2, 4, and 5. The response function for the cell with the higher concentration has less of a tendency to saturate in the range of

atmospheric concentrations considered. Therefore, the inferred concentration at any signal level is less sensitive to the small changes in the response function induced by variations in τ_A.

For a given species and cell concentration, the deviations in inferred concentration are of smaller magnitude for the Model 2 atmosphere than for the Model 1 standard. Although not illustrated in the figures, the reason for this situation is similar. The Model 2 atmosphere, with higher surface and atmospheric temperatures than Model 1, produces generally higher signal levels and leads to response functions with less of a tendency to saturate than those arising from Model 1. These "stiffer" response functions lead to lower deviations in inferred concentration with changes in τ_A.

VI. CONCLUSIONS

From the preceding discussion, it is clear that the sensitivity of the GFCR to variations in the balancing aperture is not a simple relationship. Not only do the deviations depend in a very nonlinear way on the magnitude of the deviation in τ_A, but also upon the particular spectral region or species considered, the concentration in the sample cell of the instrument, and the details of the surface and atmosphere over which the instrument is operated. In addition, for a given deviation in τ_A, there does not seem to be a consistent relationship between the level of inferred concentration and the deviation to be expected. In other words, for a particular τ_A, it is not possible to predict whether the greatest deviations in the inferred concentration will occur at high, intermediate, or low pollutant levels.

The complex dependence of the deviations notwithstanding, some general conclusions concerning optical balance from an operational point of view can be reached.

For the CO, CH_4, and the higher pressure cell of the NH_3 channel, the deviations in inferred concentration will be kept within reasonable limits, i.e., to 12 percent, if τ_A is maintained to within ± 0.1 percent of its nominal value. In view of the consistently high deviation observed for the lower pressure cell of the NH_3 channel, consideration of a higher partial pressure in this cell seems warranted. It should be noted that the above

conclusions apply to the ranges of pollutant concentrations considered in this study and may not be valid for ranges significantly different from them. Also, it is evident that atmospheric and surface conditions which tend to reduce the signal levels; e.g., lower surface temperatures, and more nearly isothermal temperature profiles, will tend to increase the deviation expected at any given deviation in τ_A. For the lower pressure cell of the NH_3 channel and for the SO_2 channel, unacceptably large deviations are much more likely to occur with ± 0.1 percent tolerance on τ_A. A rough estimate of the limits on the optical balance required to give the same probability of not exceeding about ± 12 percent deviation in concentration would be ± 0.03 percent. The same qualifications, of course, apply as did to the other species; in fact, the sensitivity of the required tolerance to surface and atmospheric parameters may be even stronger in the case of the lower pressure cell of NH_3 and of SO_2 than for the other species considered.

REFERENCES

1. Ludwig, C. B.; Bartle, R.; and Griggs, M.: Study of Air Pollution Detection by Remote Sensors. NASA CR-1380, July 1969.

2. Ludwig, C. B.; Griggs, M.; Malkmus, W.; and Bartle, E. R.: Air Pollution Measurements from Satellites. NASA CR-2324, November 1973.

3. Science Applications, Incorporated: Monitoring of Air Pollution by Satellites. Monthly Progress Report No. 8, Contract No. NAS1-12048, La Jolla, CA 92037, September 1, 1973.

4. Committee on Extension to the Standard Atmosphere: U. S. Standard Atmosphere, 1962. U. S. Government Printing Office, Washington, D. C., December 1962.

5. Gutnick, Murray: Aids for Computing Stratospheric Moisture. Geophysics Research Directorate Research Notes No. 50. Air Force Cambridge Research Laboratories, AFCRL 203, Bedford, MA 01730, 1961.

6. Committee on Extension to the Standard Atmosphere: U. S. Standard Atmosphere Supplements, 1966. U. S. Government Printing Office, Washington, D. C., 1966.

7. McClatchey, R. A.; Fenn, R. W.; Seldy, J. E. V.; Volz, F. E.; and Garing J. S.: Optical Properties of the Atmosphere (Third Edition). Air Force Cambridge Research Laboratories, AFCRL 72-0497, Bedford, MA 01730, August 1972.

Table 1

INSTRUMENT PARAMETERS

Parameter \ Species	CO	SO_2	NH_3	CH_4
Center Wavelength (micrometers)	4.66	8.55	11.2	8.0
Bandwidth (micrometers)	4.50 - 4.32	8.11 - 8.99	10.43 - 11.97	7.53 - 8.47
Cell Pressure (N/m^2)	1.013×10^5	1.013×10^5	1.013×10^5	1.013×10^5
Cell Length (cm)	1	1	1	1
Partial Pressure (N/m^2)				
Cell 1	3.546×10^4	1.013×10^5	2.026×10^4	1.013×10^5
Cell 2	1.013×10^4		1.013×10^3	2.026×10^4
Cell Temperature (K)	300	300	300	300
Balance Temperature (K)				
Cold	266	266	266	266
Hot	310	310	310	310
Standard Aperture Transmission (τ_A)				
Cell 1	.830128	.514679	.849515	.754904
Cell 2	.915968		.982169	.904845

Table 2

DETAILS OF ATMOSPHERIC MODELS

Model	Layer	Extent (km)	Pressure (N/m^2)	Temperature (K)	I.R.-Active Constituent Concentrations (ppm)						
					CO_2	H_2O	N_2O	CO	SO_2	CH_4	NH_3
1	1	0 - 2	9.142×10^4	282.02	330.	6254.	.28	.1	.005	1.	.01
	2	2 - 4	7.136	269.11	330.	3408.	.28	.1	.005	1.	.01
	3	4 - 7	5.169	253.34	330.	1335.	.28	.1	.005	1.	.01
	4	7 - 11	3.176	231.26	330.	274.	.28	.1	.005	1.	.01
	5	11 - 22	9.555×10^3	216.97	330.	15.	.28	.1	.005	1.	.01
2	1	0 - 2	9.048×10^4	291.30	330.	14310.	.28	.5	.06	1.	.01
	2	2 - 4	7.126	280.00	330.	6529.	.28	.2	.005	1.	.01
	3	4 - 7	5.224	264.80	330.	2143.	.28	.1	.005	1.	.01
	4	7 - 11	3.279	242.80	330.	504.3	.28	.1	.005	1.	.01
	5	11 - 22	1.164	218.60	330.	17.84	.28	.1	.005	1.	.01

APPENDIX A

Deviations in inferred concentration as function of atmospheric model, species, cell partial pressure, and pollutant concentration, and deviations in τ_A

Model	Species	Cell Partial Pressure (N/m^2)	Standard Pollutant Concentration (ppm)	$\Delta \tau_A$ Percent					
				-1	-.1	-.01	+.01	+.1	+1
1	CO	3.546×10^4	.05	-80.0	-8.0	-1.0	3.0	10.0	50.0
			.1	-70.0	-6.0	-.5	5.0	6.0	42.0
			.2	-66.0	-5.0	-1.3	1.0	6.0	40.0
			.3	-66.7	-5.3	-.7	.7	6.7	38.7
		1.013×10^4	.05	-152.0	-12.0	-2.0	2.0	7.0	70.0
			.1	-140.0	-10.0	-2.0	.5	4.0	60.0
			.2	-177.0	-10.3	-.5	1.0	7.0	56.0
			.3	-217.0	-9.3	-.3	2.0	9.7	57.0
	SO_2	1.013×10^5	.005	*	-70.0	- 8.0	4.0	68.0	*
			.0075	*	-44.0	- 5.3	2.7	42.7	*
			.01	*	-28.0	- 2.0	4.0	35.0	*
			.015	*	-25.3	- 2.7	2.0	26.7	*
	CH_4	1.013×10^5	.5	- 28.0	- 5.0	- 2.0	2.0	4.0	18.0
			1.0	- 27.0	- 3.0	- 1.0	1.0	3.0	20.0

Model	Species	Cell Partial Pressure (N/m^2)	Standard Pollutant Concentration (ppm)	$\Delta \tau_A$ Percent					
				-1	-.1	-.01	+.01	+.1	+1
1 (Cont.)	CH_4 (cont'd)	1.013×10^5	1.5	- 26.7	- 2.7	- .7	.7	3.3	20.0
			2.0	- 32.0	- 2.0	- .5	.5	2.0	20.5
		2.026×10^4	.5	- 76.0	- 8.0	-4.0	2.0	4.0	42.0
			1.0	-102.0	- 7.0	-2.0	1.0	4.0	41.0
			1.5	-133.0	- 7.3	- .7	1.3	6.7	44.0
			2.0	-110.0	- 5.0	- 1.0	1.0	8.0	48.0
	NH_3	2.026×10^4	.005	- 88.0	- 8.0	- 2.0	2.0	6.0	78.0
			.01	- 52.0	- 4.0	- 1.0	1.0	5.0	45.0
			.02	- 31.5	- 2.5	- .5	.5	3.5	28.0
			.025	- 28.4	- 2.8	- .4	.4	2.4	24.4
		1.013×10^3	.005	*	-40.0	- 4.0	2.0	38.0	*
			.01	*	-24.0	- 2.0	3.0	26.0	*
			.02	*	-14.5	- 1.5	2.0	19.5	*
			.025	*	-13.2	- .8	1.6	17.6	*

APPENDIX A (Cont.)

Model	Species	Cell Partial Pressure (N/m^2)	Standard Pollutant Concentration (ppm)	$\Delta \tau_A$ Percent					
				-1	-.1	-.01	+.01	+.1	+1
2	CO	3.546×10^4	.05	-40.0	-4.0	-2.0	2.0	4.0	28.0
			.1	-33.0	-3.0	-1.0	2.0	4.0	24.0
			.2	-32.0	-2.0	-.5	1.0	3.0	24.5
			.3	-31.7	-2.0	-.7	1.3	3.0	18.0
	CO	1.013×10^4	.05	-68.0	-4.0	-2.0	2.0	12.0	44.0
			.1	-64.0	-7.0	-2.0	1.0	3.0	38.0
			.2	-70.0	-8.0	-1.0	.5	1.0	36.0
			.3	-90.0	-3.3	.3	1.7	7.0	40.0
	SO_2	1.013×10^5	.005	-292.0	-30.0	- 4.0	2.0	24.0	*
			.0075	-194.7	-18.7	- 2.7	1.3	17.3	*
			.01	-148.0	-15.0	- 2.0	1.0	13.0	*
			.015	-100.7	-10.7	- 1.3	.7	8.7	*
	CH_4	1.013×10^5	.5	- 18.0	- 4.0	- 2.0	2.0	4.0	12.0
			1.0	- 18.0	- 3.0	- 1.0	1.0	2.0	12.0
			1.5	- 16.0	- 2.0	- .7	.7	2.7	13.3

APPENDIX A (Concl.)

Model	Species	Cell Partial Pressure (N/m^2)	Standard Pollutant Concentration (ppm)	$\Delta \tau_A$ Percent					
				-1	-.1	-.01	+.01	+.1	+1
2 (Cont.)	CH_4 (Cont.)	1.013×10^5	2.0	- 15.5	- 1.5	- .5	.5	2.5	15.5
		2.026×10^4	.5	- 44.0	- 6.0	- 2.0	2.0	4.0	30.0
			1.0	- 53.0	- 4.0	- 1.0	1.0	4.0	28.0
			1.5	- 62.7	- 4.7	- 1.3	1.3	4.7	31.3
			2.0	- 78.5	- 2.5	- 1.0	1.3	5.5	34.0
	NH_3	2.026×10^4	.005	- 34.0	- 6.0	- 2.0	2.0	4.0	32.0
			.01	- 21.0	- 3.0	- 1.0	1.0	2.0	19.0
			.02	- 13.0	- 1.5	- .5	.5	1.0	12.0
			.025	- 11.6	- 1.2	- .4	.4	.8	10.8
		1.013×10^3	.005	*	-18.0	- 2.0	2.0	14.0	*
			.01	*	- 9.0	- 1.0	2.0	10.0	*
			.02	*	- 6.5	- 1.0	1.0	5.5	*
			.025	*	- 5.6	- .4	.4	6.0	*

*For these values of the parameters, the response functions of the instrument remained below the radiance levels used to infer concentrations.

APPENDIX B

SYMBOLS

$C(\nu)$	transfer function of the total optical path through the gas cell at wavenumber ν
$C'(\nu)$	transfer function of the total optical path through the vacuum cell at wavenumber ν
$E(\nu)$	radiance incident on the instrument at wavenumber ν (watts/cm^2 · sr cm^{-1})
N	average of radiances passing through the vacuum cell and gas cell, integrated over wavenumber (watts/cm^2 sr)
ΔN	difference between radiances passing through vacuum cell and gas cell integrated over wavenumber (watts/cm^2 sr)
V	instrument output signal corresponding to N (volts)
ΔV	instrument output signal corresponding to ΔN (volts)
τ_A	transmissivity of the vacuum cell aperture, optical balance parameter (see fig. 1)
$\tau_G(\nu)$	transmittance of the gas cell at wavenumber ν
ν	wavenumber (cm^{-1})
$\Delta\nu$	bandpass of the filter (cm^{-1}) (see fig. 1)

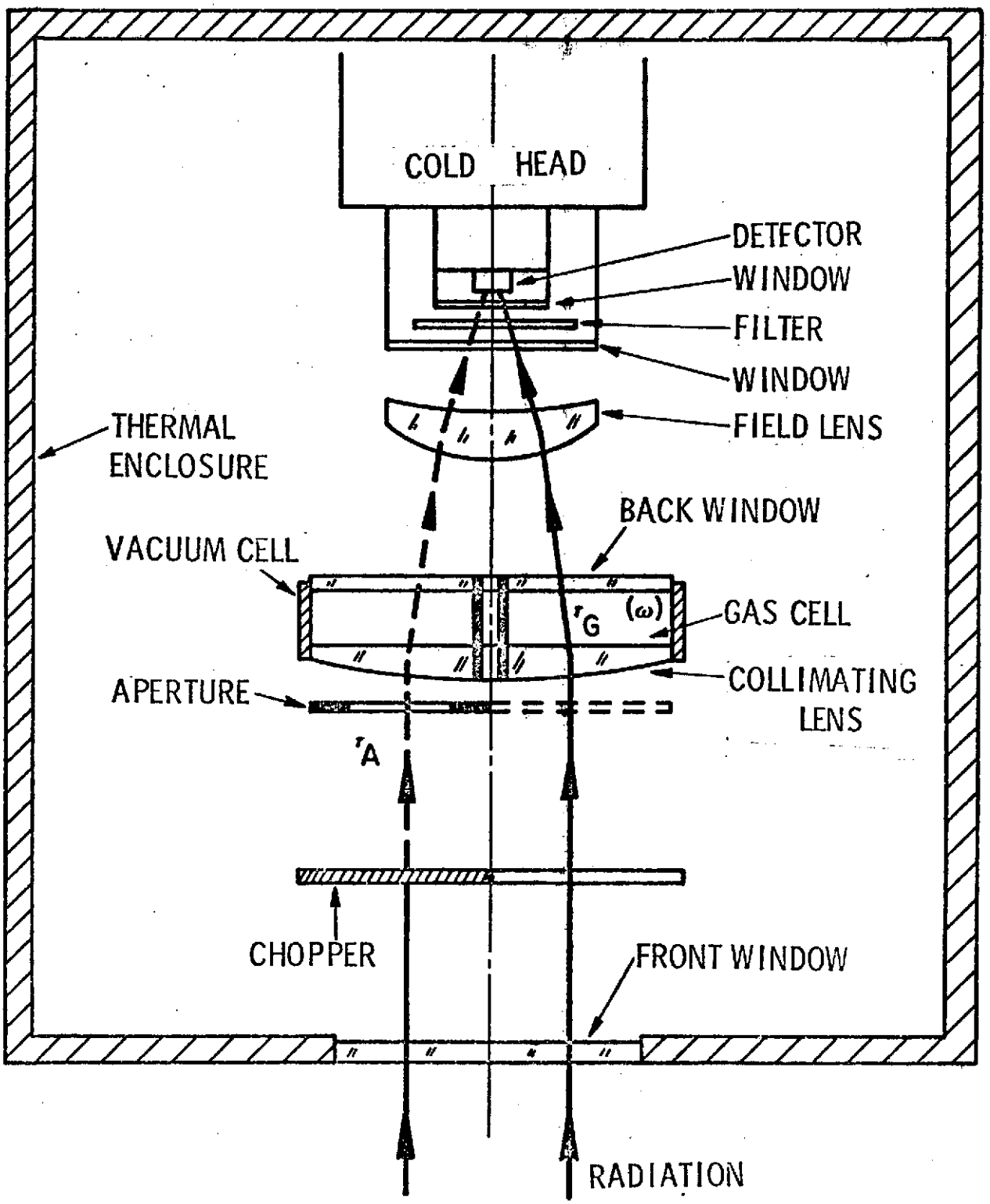

Figure 1. - Schematic of typical Gas Filter Correlation Radiometer.

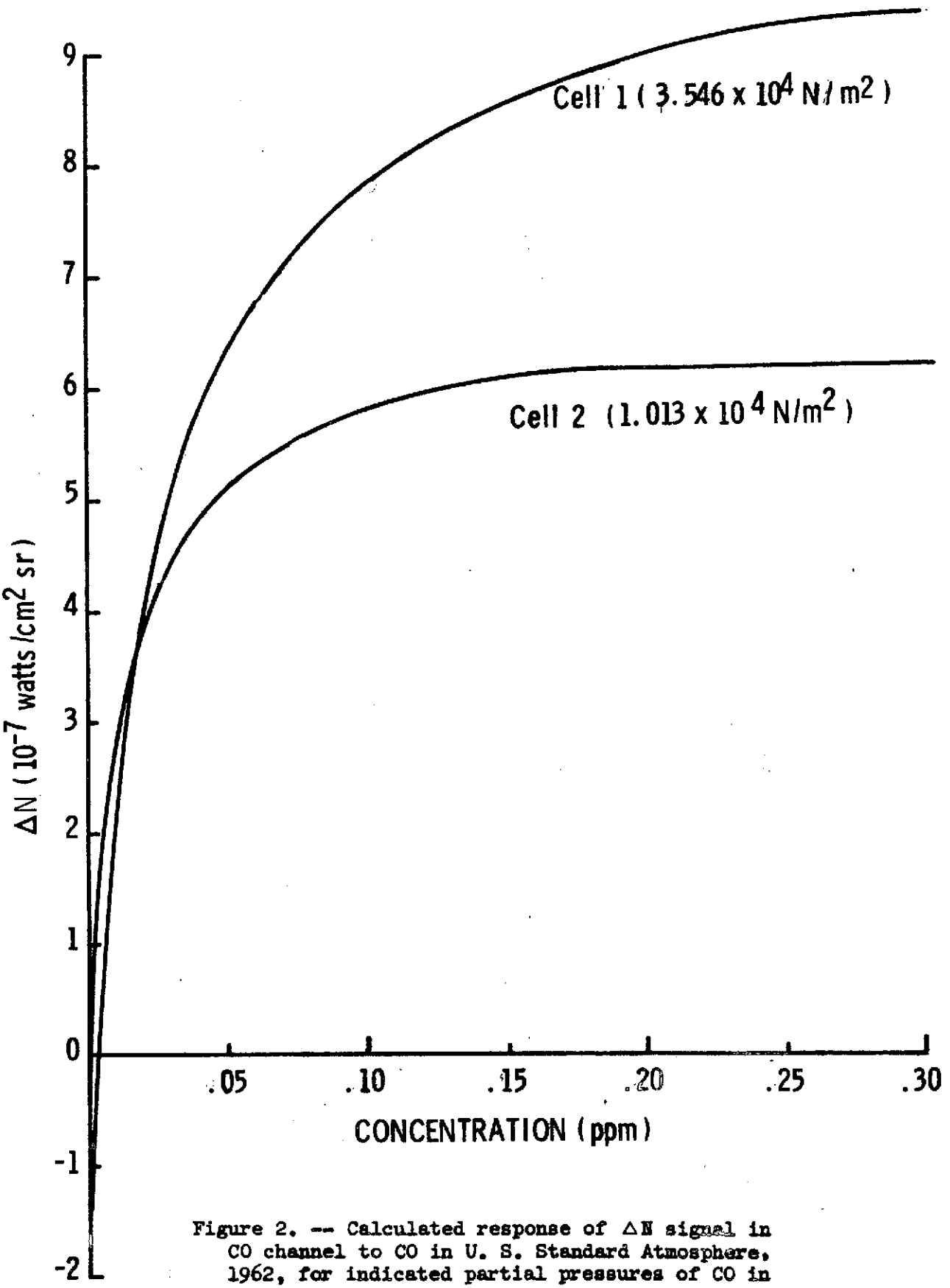

Figure 2. -- Calculated response of ΔN signal in CO channel to CO in U. S. Standard Atmosphere, 1962, for indicated partial pressures of CO in instrument gas cell.

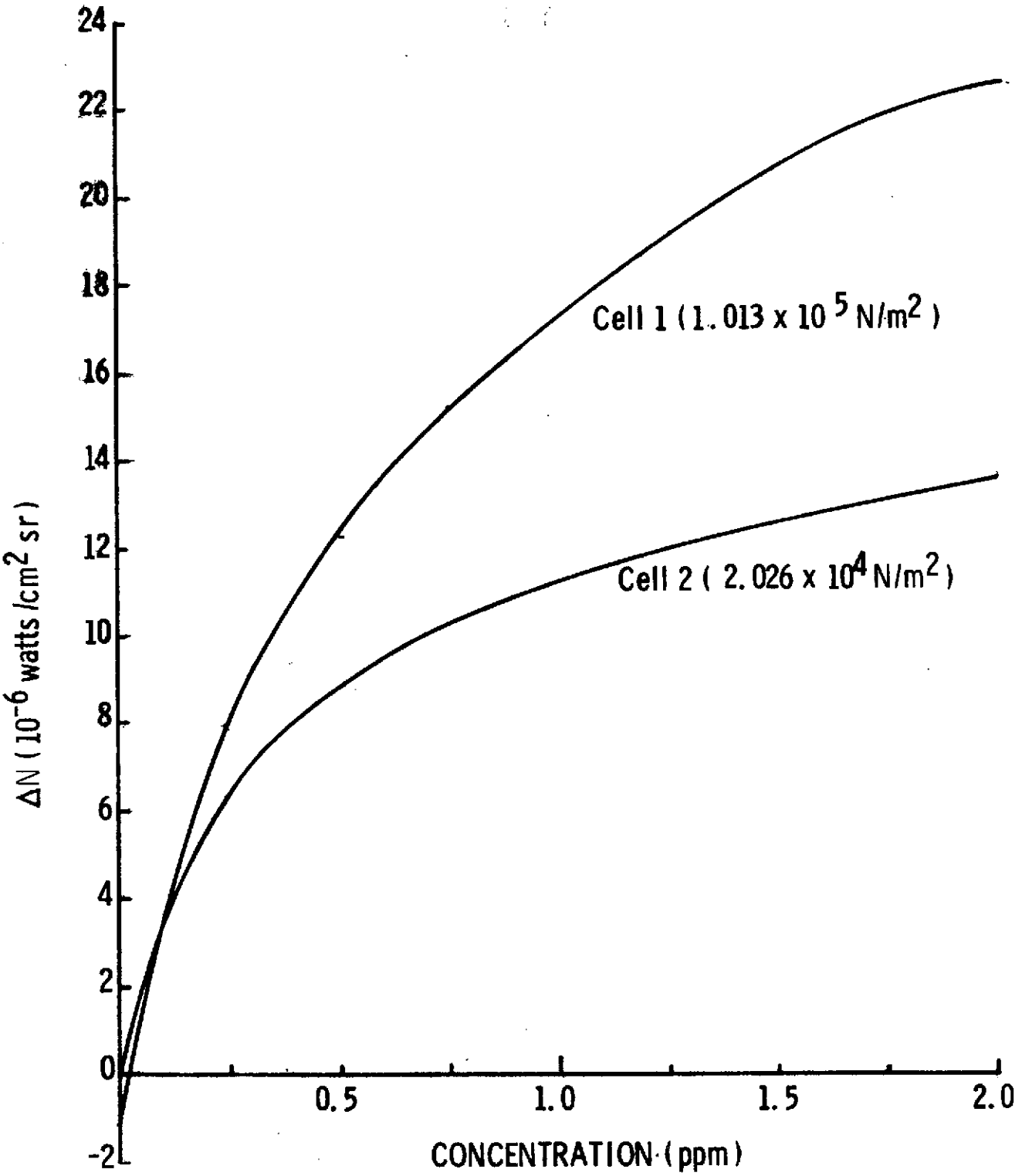

Figure 3. -- Calculated response of ΔN signal in CH_4 channel to CH_4 in U. S. Standard Atmosphere, 1962, for indicated partial pressures of CH_4 in instrument gas cell.

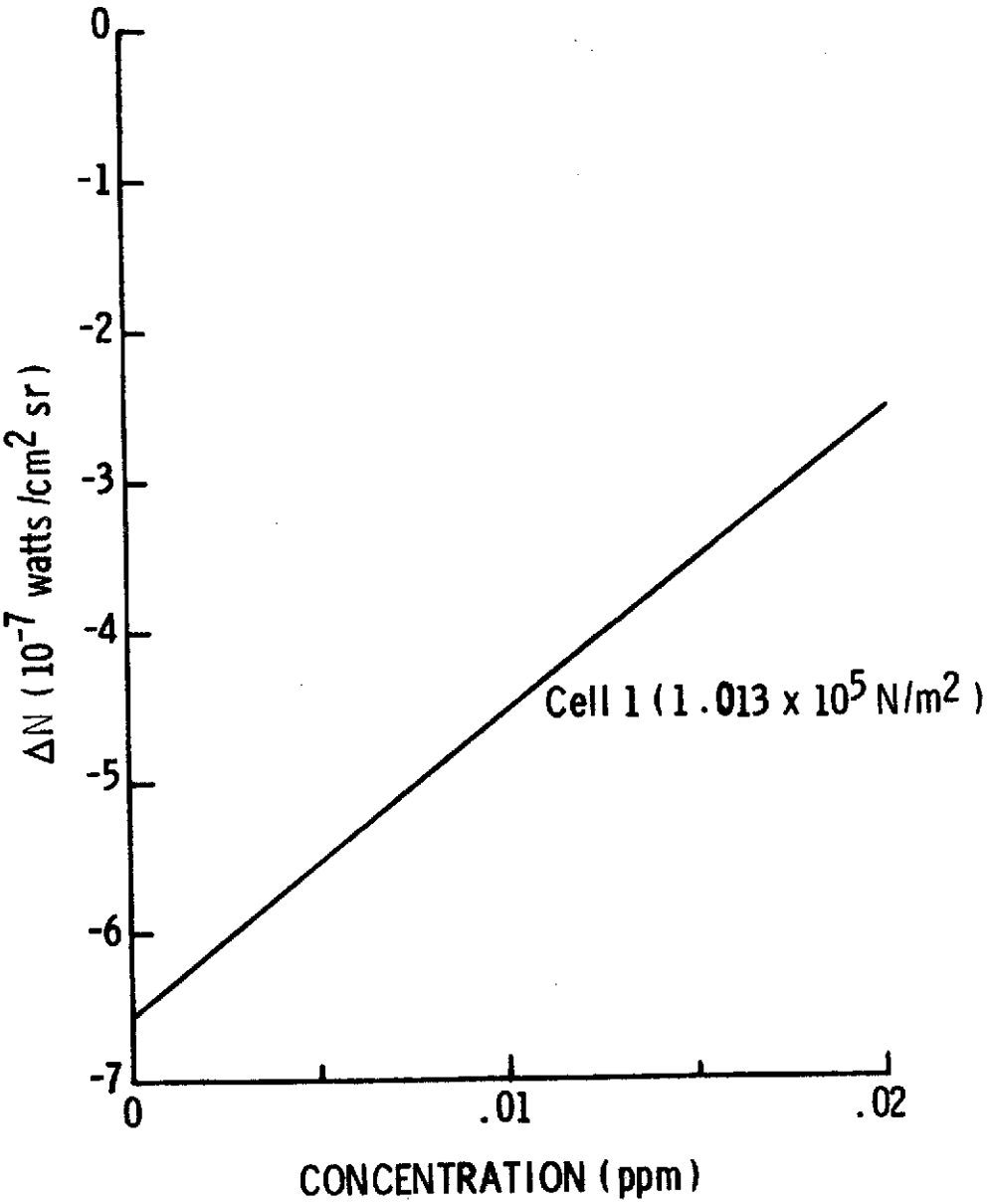

Figure 4. -- Calculated response of ΔN signal in SO_2 channel to SO_2 in U. S. Standard Atmosphere, 1962, for indicated partial pressure of SO_2 in instrument gas cell.

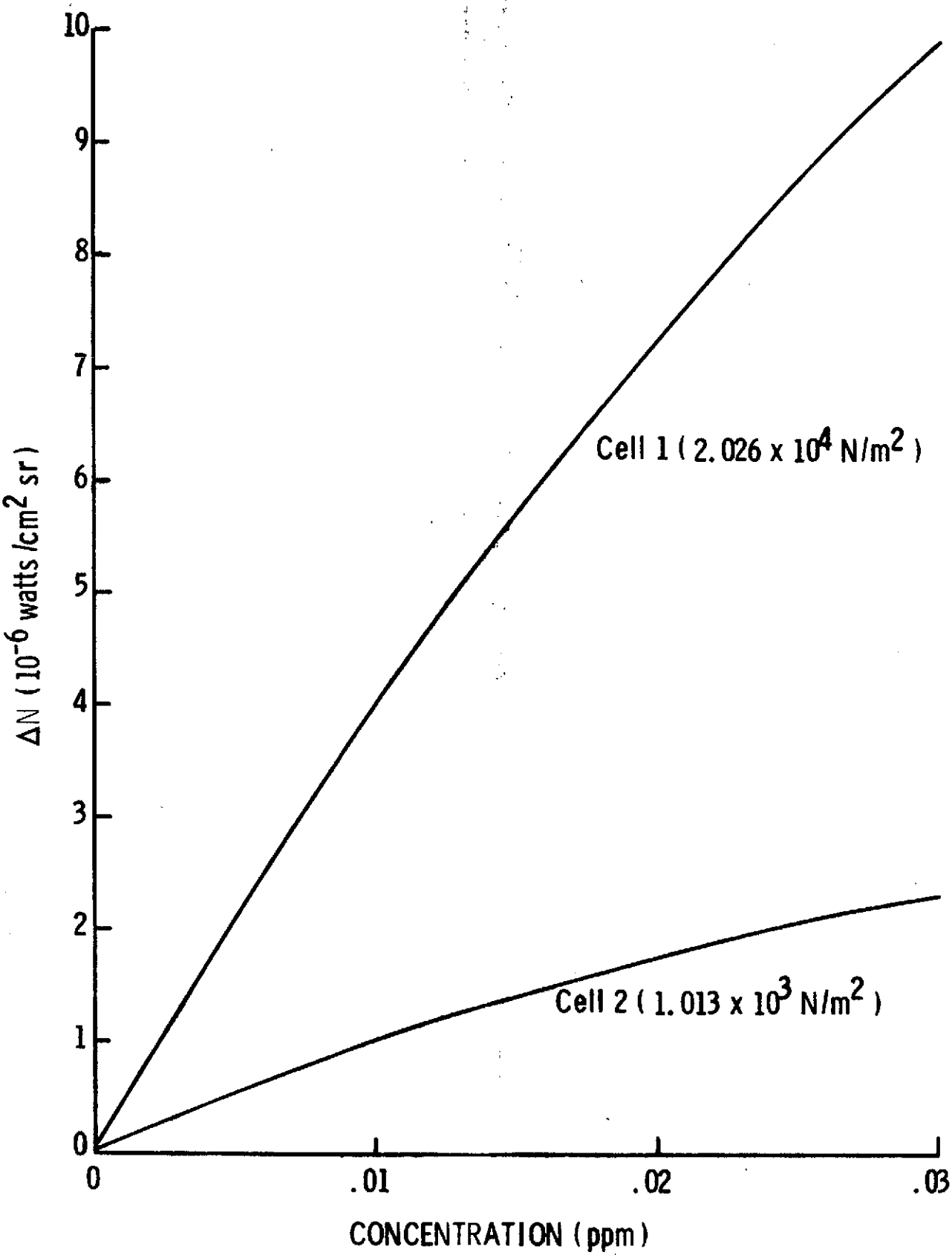

Figure 5. -- Calculated response of ΔN signal in NH_3 channel to NH_3 in U. S. Standard Atmosphere, 1962, for indicated partial pressures of NH_3 in instrument gas cell.

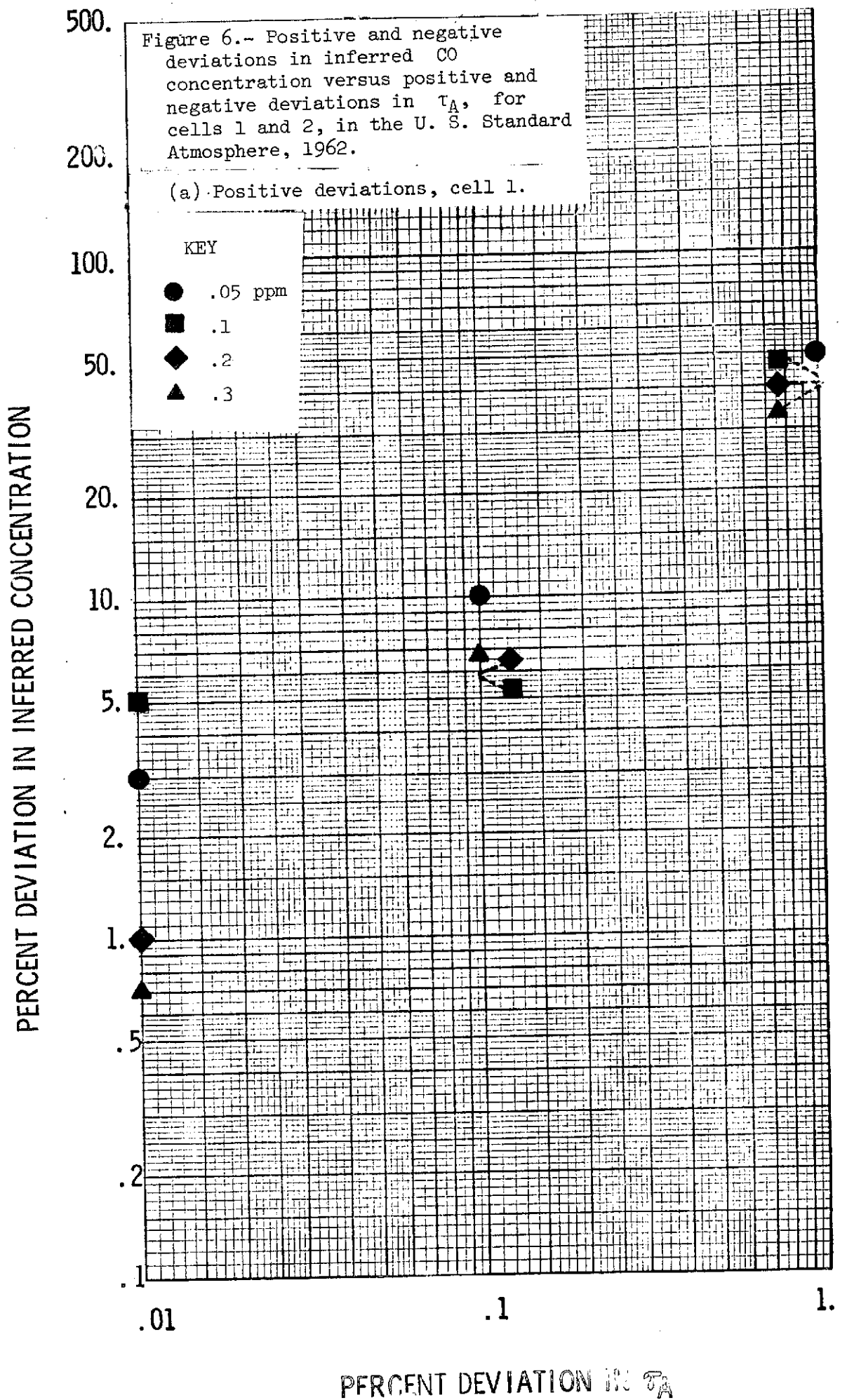
Figure 6.- Positive and negative deviations in inferred CO concentration versus positive and negative deviations in τ_A, for cells 1 and 2, in the U. S. Standard Atmosphere, 1962.
(a) Positive deviations, cell 1.
KEY
.05 ppm
.1
.2
.3
500.
200.
100.
50.
20.
10.
5.
2.
1.
.5
.2
.1
.01
.1
1.
PERCENT DEVIATION IN INFERRED CONCENTRATION
PERCENT DEVIATION IN τ_A

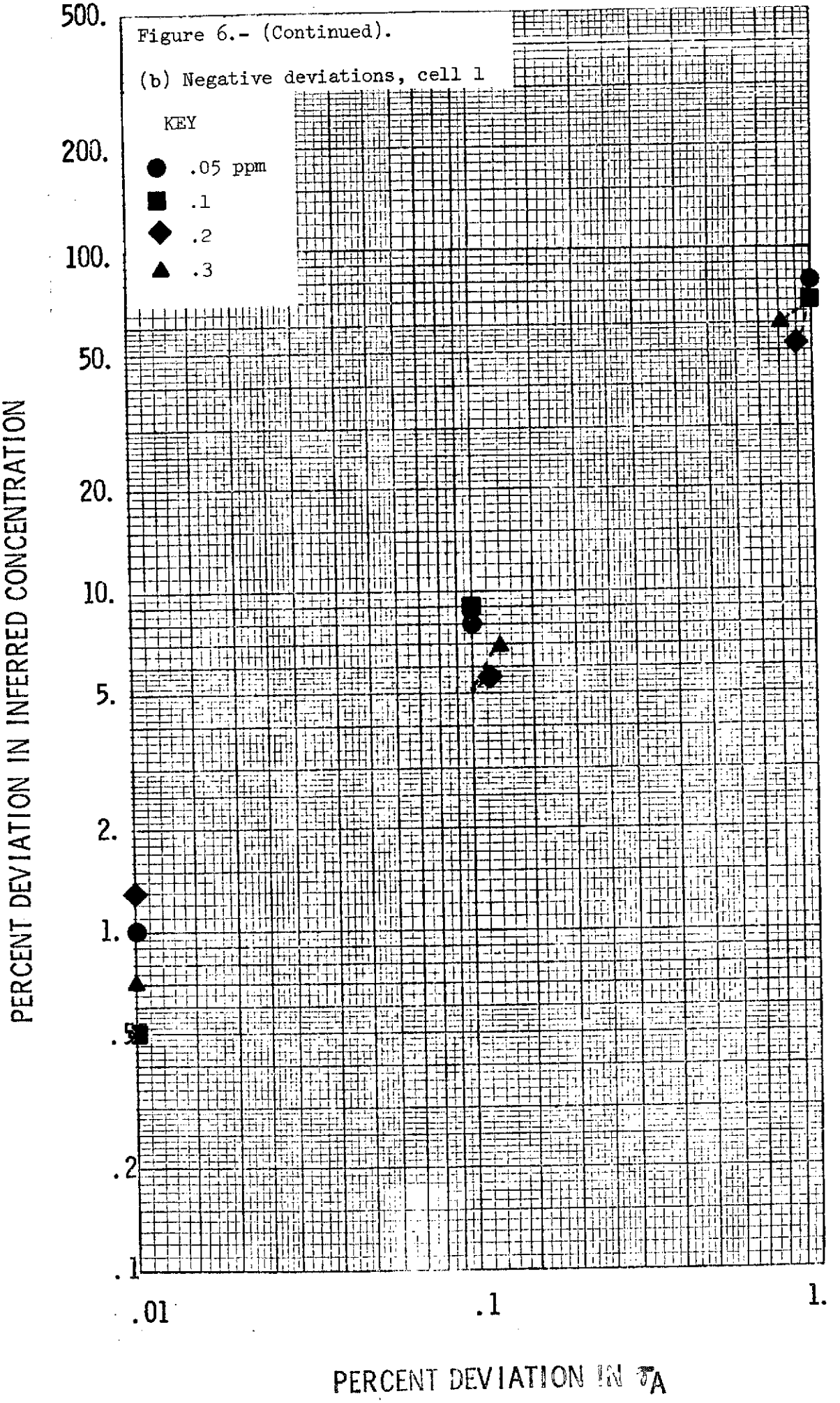
Figure 6.- (Continued).
(b) Negative deviations, cell 1
KEY
.05 ppm
.1
.2
.3
500.
200.
100.
50.
20.
10.
5.
2.
1.
.5
.2
.1
.01
.1
1.
PERCENT DEVIATION IN INFERRED CONCENTRATION
PERCENT DEVIATION IN $\bar{\tau}_A$

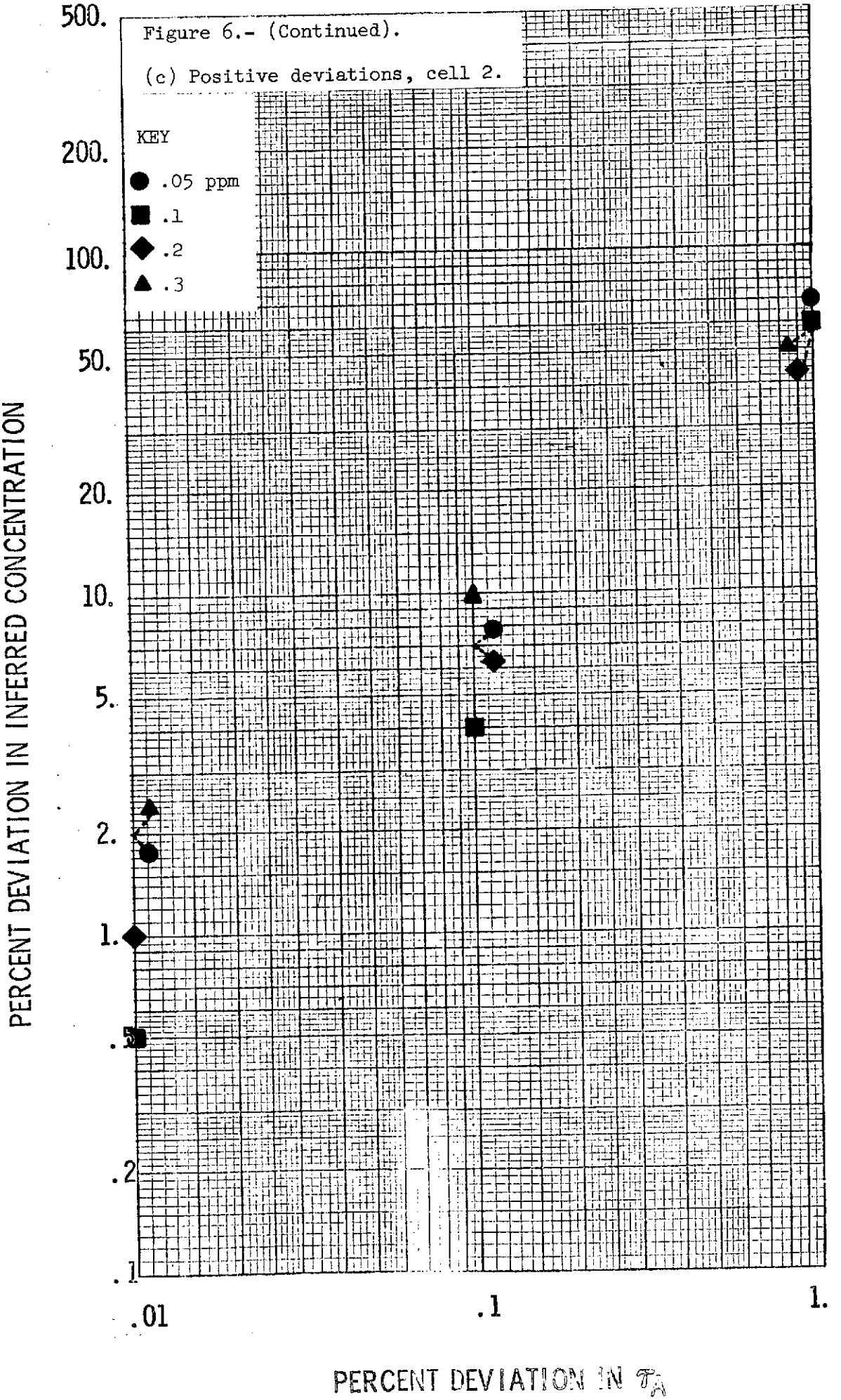
Figure 6.- (Continued).
(c) Positive deviations, cell 2.
KEY
.05 ppm
.1
.2
.3
500.
200.
100.
50.
20.
10.
5.
2.
1.
.5
.2
.1
.01
.1
1.
PERCENT DEVIATION IN INFERRED CONCENTRATION
PERCENT DEVIATION IN T_A

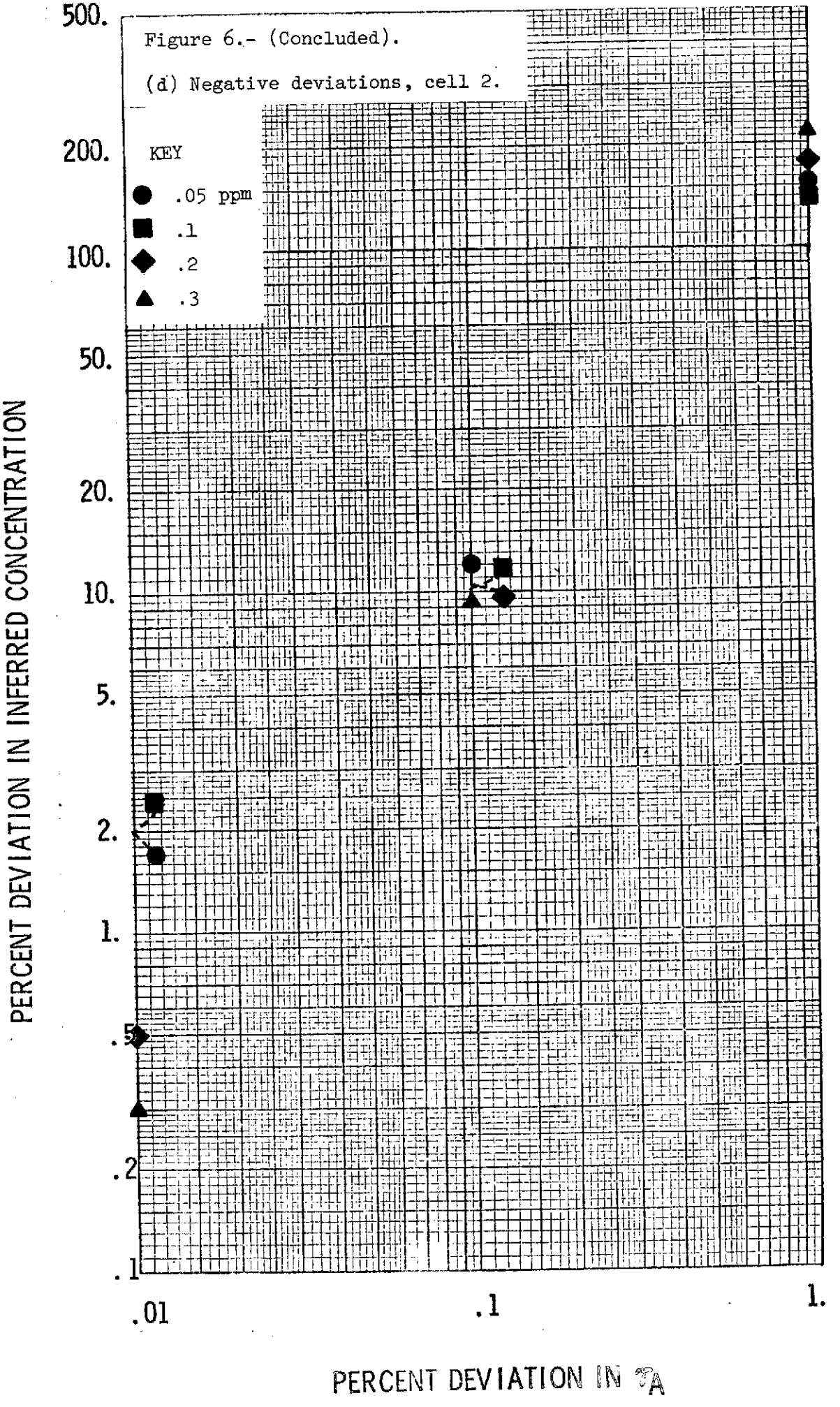
Figure 6.- (Concluded).
(d) Negative deviations, cell 2.
KEY
.05 ppm
.1
.2
.3
500.
200.
100.
50.
20.
10.
5.
2.
1.
.5
.2
.1
.01
.1
1.
PERCENT DEVIATION IN INFERRED CONCENTRATION
PERCENT DEVIATION IN

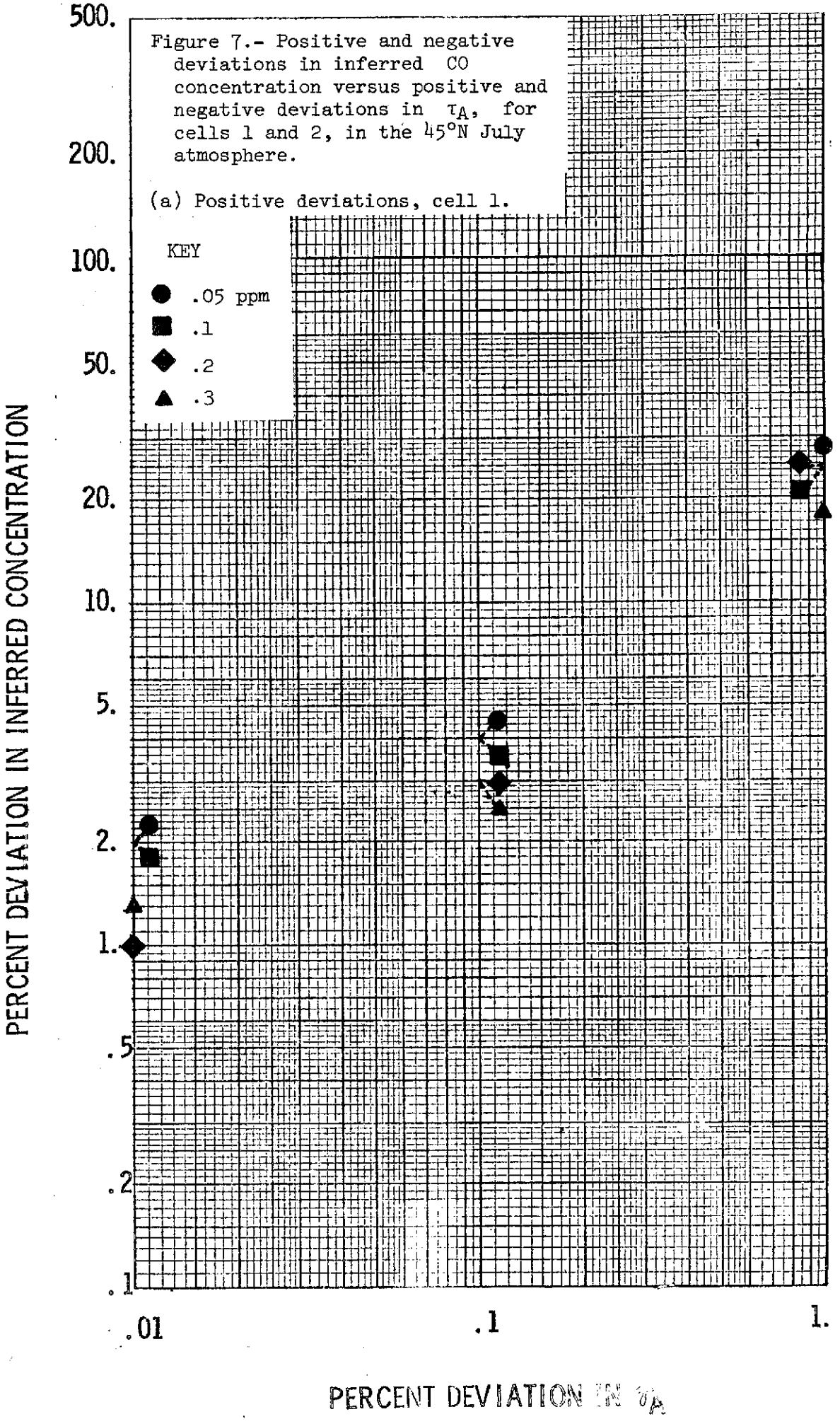
Figure 7.- Positive and negative deviations in inferred CO concentration versus positive and negative deviations in τ_A, for cells 1 and 2, in the 45°N July atmosphere.
(a) Positive deviations, cell 1.
KEY
.05 ppm
.1
.2
.3
500.
200.
100.
50.
20.
10.
5.
2.
1.
.5
.2
.1
.01
.1
1.
PERCENT DEVIATION IN INFERRED CONCENTRATION
PERCENT DEVIATION IN τ_A

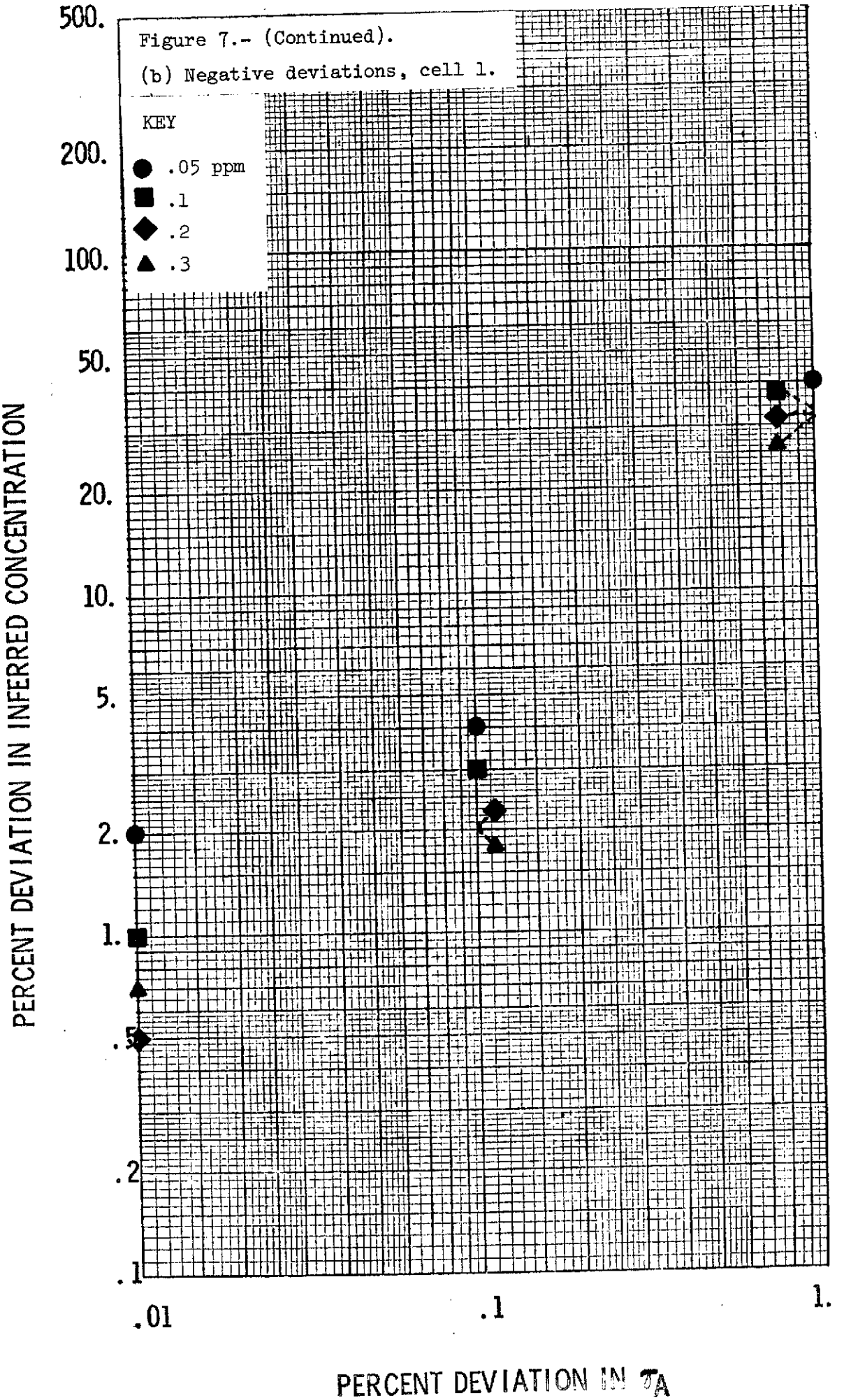
Figure 7.- (Continued).
(b) Negative deviations, cell 1.
KEY
.05 ppm
.1
.2
.3
500.
200.
100.
50.
20.
10.
5.
2.
1.
.5
.2
.1
.01
.1
1.
PERCENT DEVIATION IN INFERRED CONCENTRATION
PERCENT DEVIATION IN τ_A

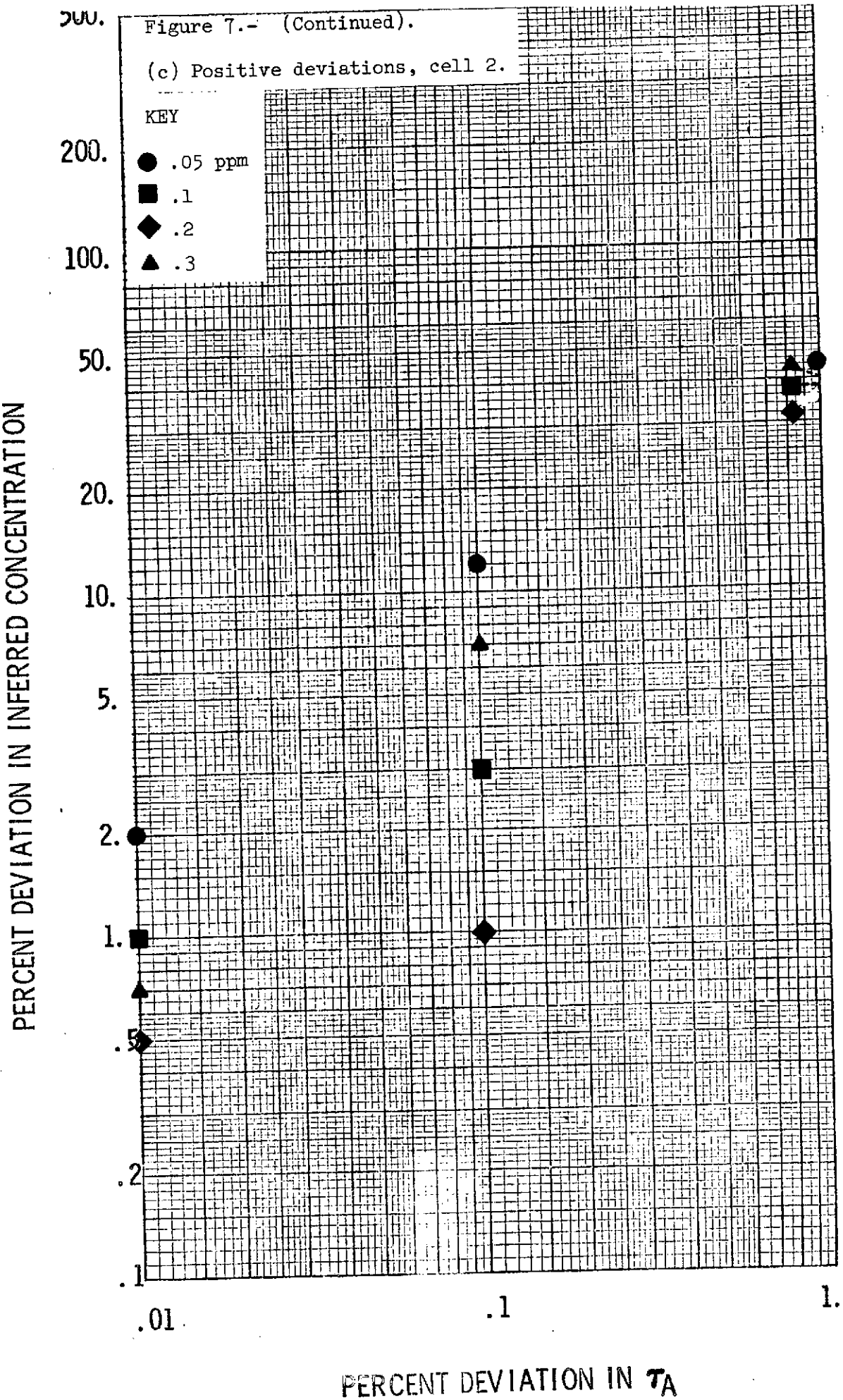
Figure 7.- (Continued).
(c) Positive deviations, cell 2.
KEY
.05 ppm
.1
.2
.3
500.
200.
100.
50.
20.
10.
5.
2.
1.
.5
.2
.1
.01
.1
1.
PERCENT DEVIATION IN INFERRED CONCENTRATION
PERCENT DEVIATION IN τ_A

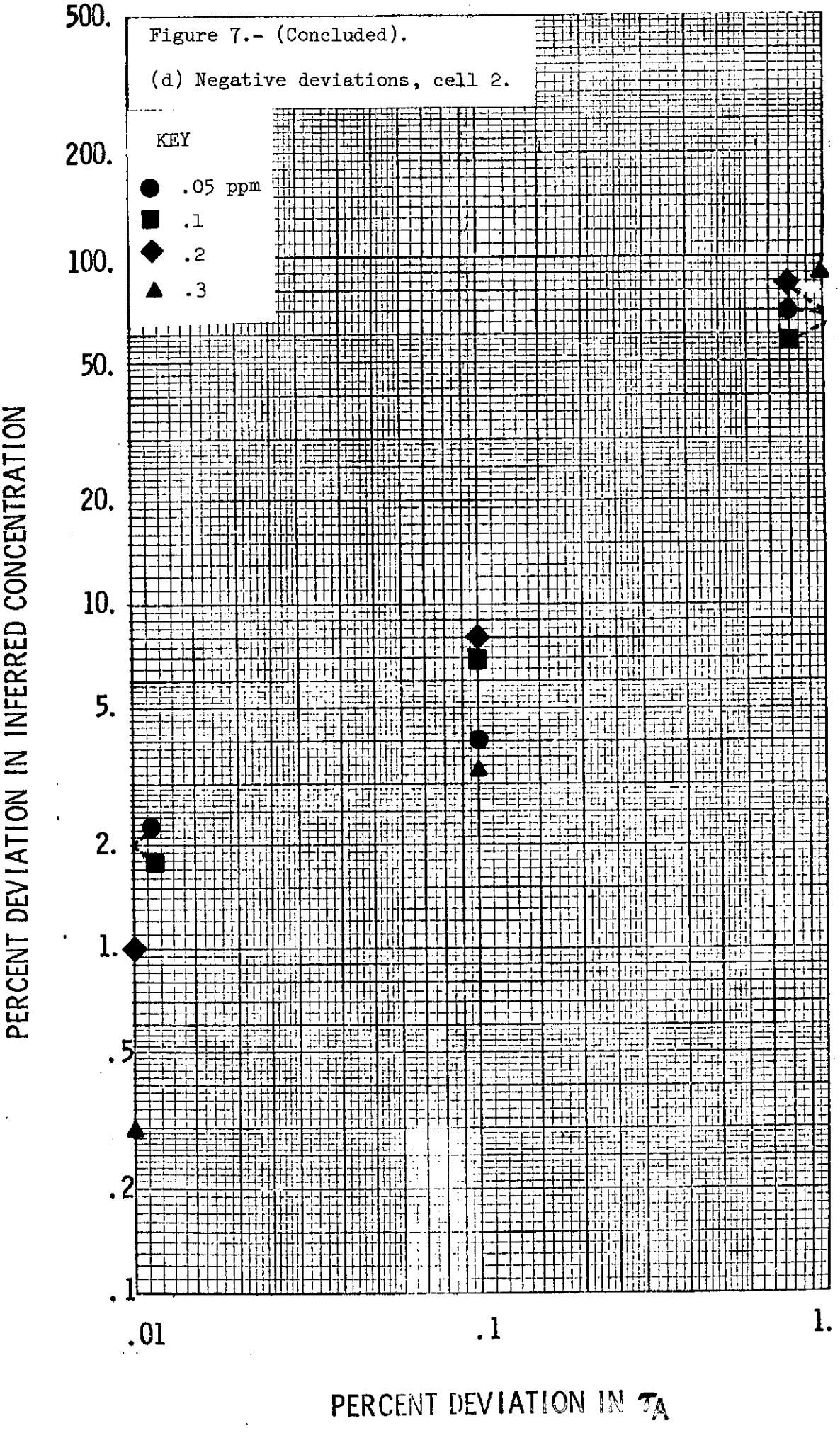
Figure 7.- (Concluded).
(d) Negative deviations, cell 2.
KEY
.05 ppm
.1
.2
.3
500.
200.
100.
50.
20.
10.
5.
2.
1.
.5
.2
.1
.01
.1
1.
PERCENT DEVIATION IN INFERRED CONCENTRATION
PERCENT DEVIATION IN τ_A

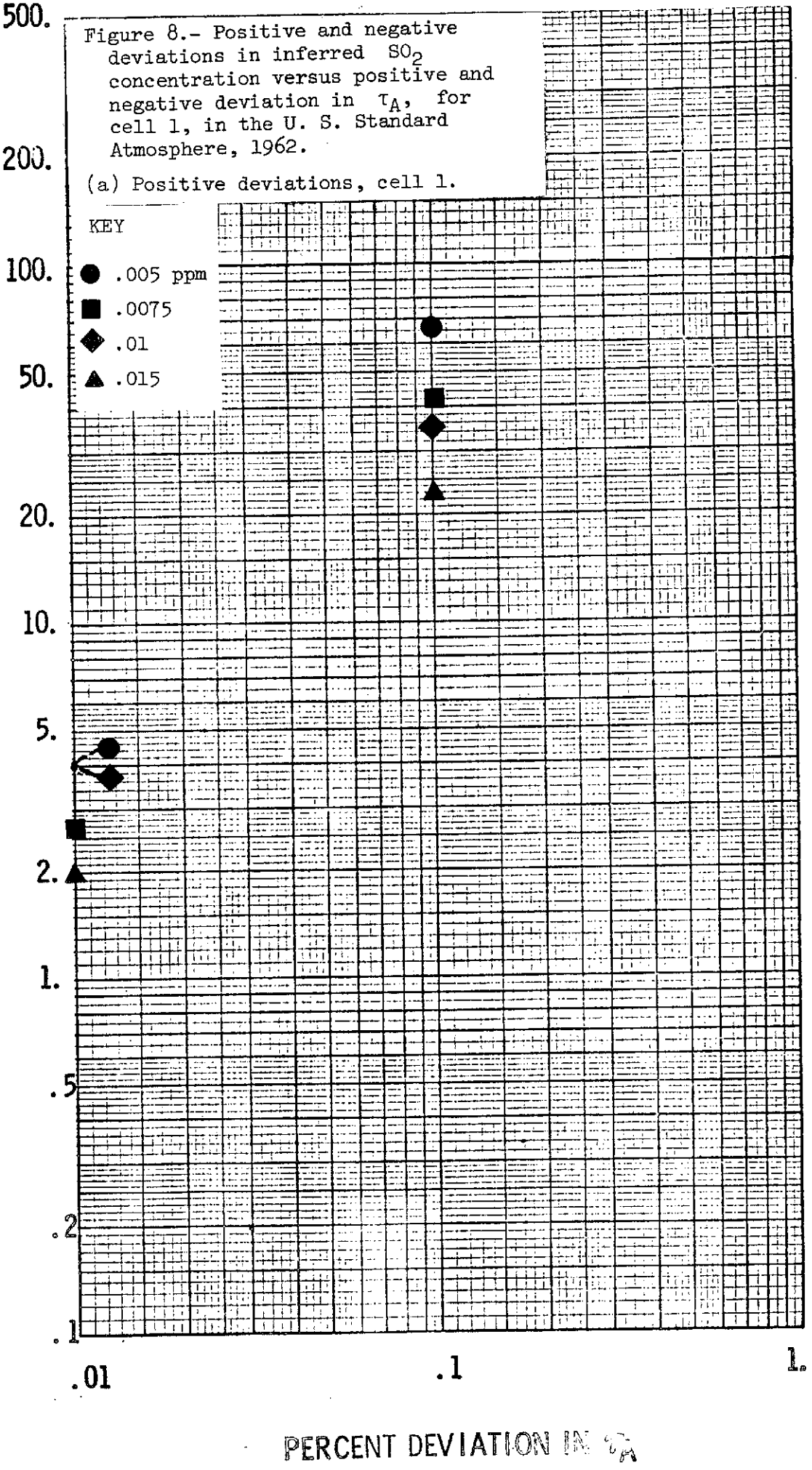

Figure 8.- Positive and negative deviations in inferred SO_2 concentration versus positive and negative deviation in τ_A, for cell 1, in the U. S. Standard Atmosphere, 1962.

(a) Positive deviations, cell 1.

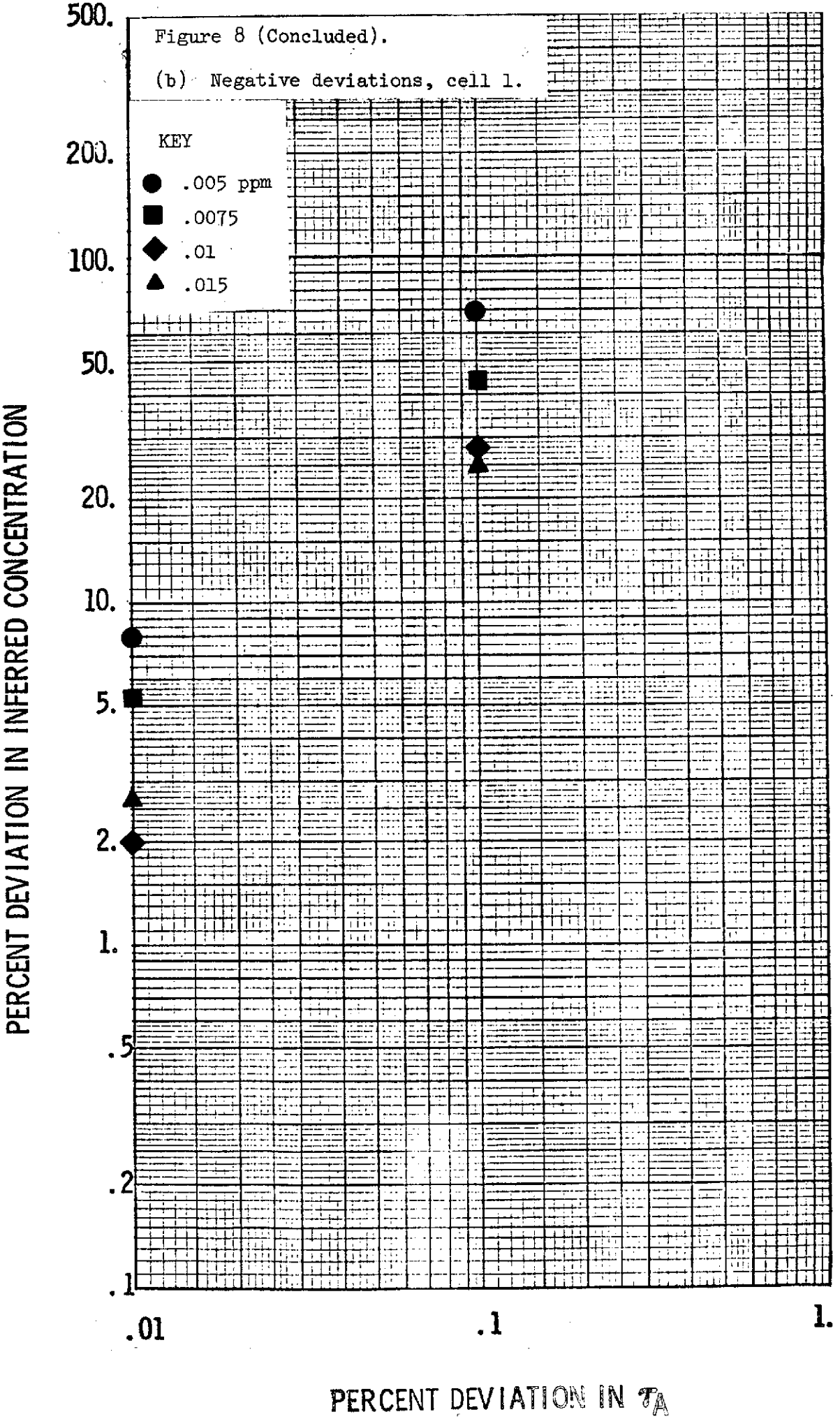
Figure 8 (Concluded).
(b) Negative deviations, cell 1.
KEY
.005 ppm
.0075
.01
.015
500.
200.
100.
50.
20.
10.
5.
2.
1.
.5
.2
.1
.01
.1
1.
PERCENT DEVIATION IN INFERRED CONCENTRATION
PERCENT DEVIATION IN T_A

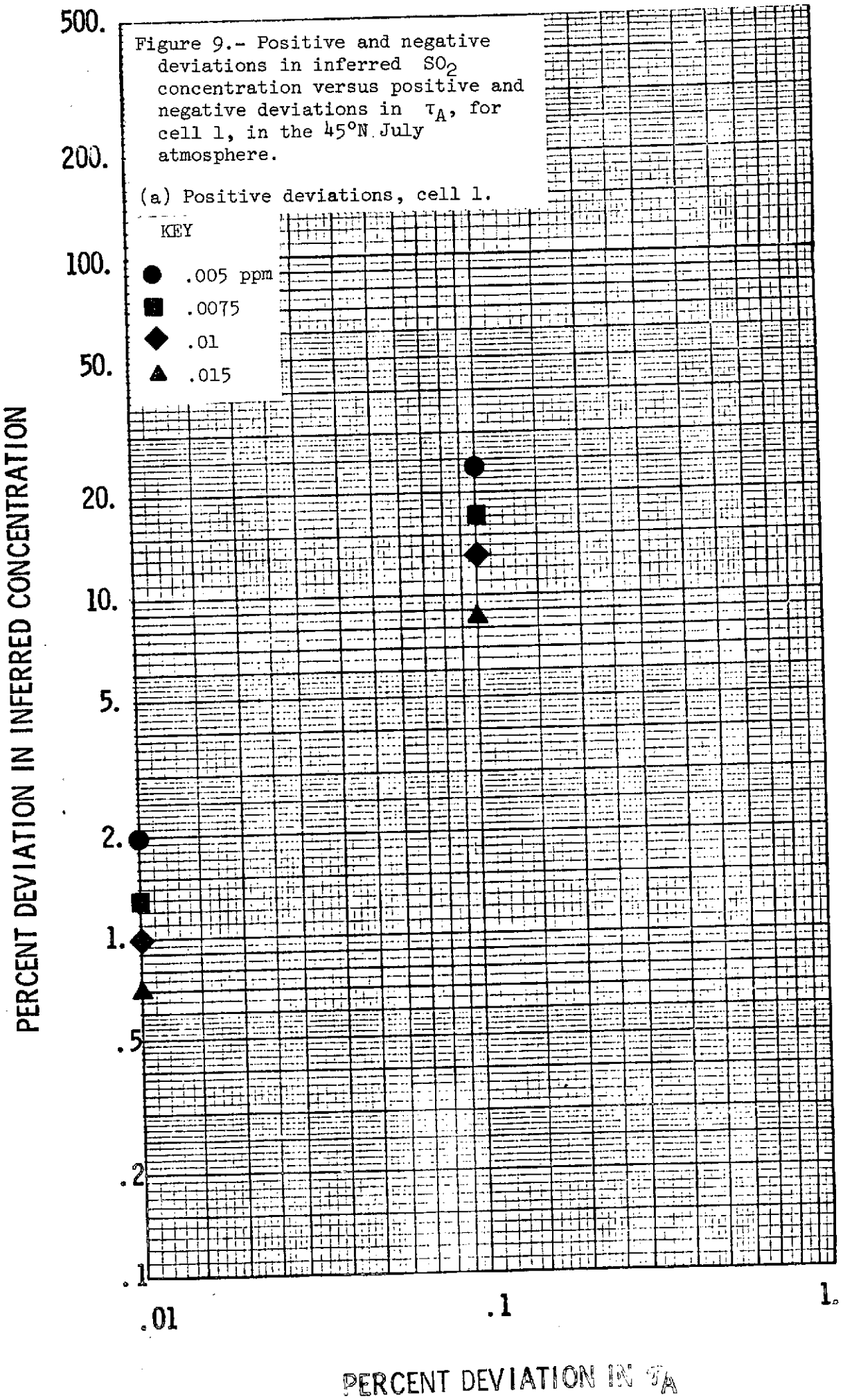

Figure 9.- Positive and negative deviations in inferred SO_2 concentration versus positive and negative deviations in τ_A, for cell 1, in the 45°N July atmosphere.

(a) Positive deviations, cell 1.

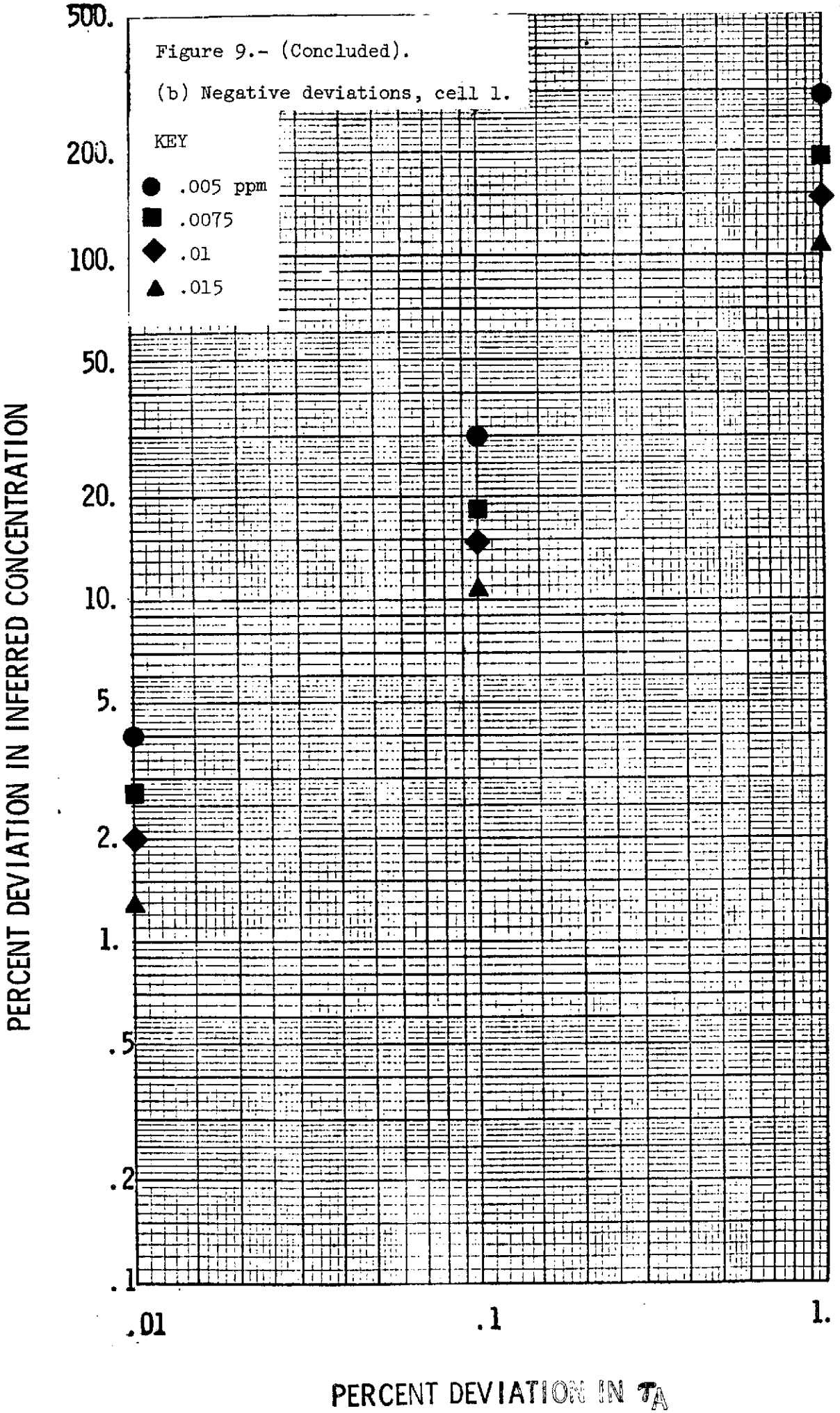
Figure 9.- (Concluded).
(b) Negative deviations, cell 1.
KEY
.005 ppm
.0075
.01
.015
500.
200.
100.
50.
20.
10.
5.
2.
1.
.5
.2
.1
.01
.1
1.
PERCENT DEVIATION IN INFERRED CONCENTRATION
PERCENT DEVIATION IN T_A

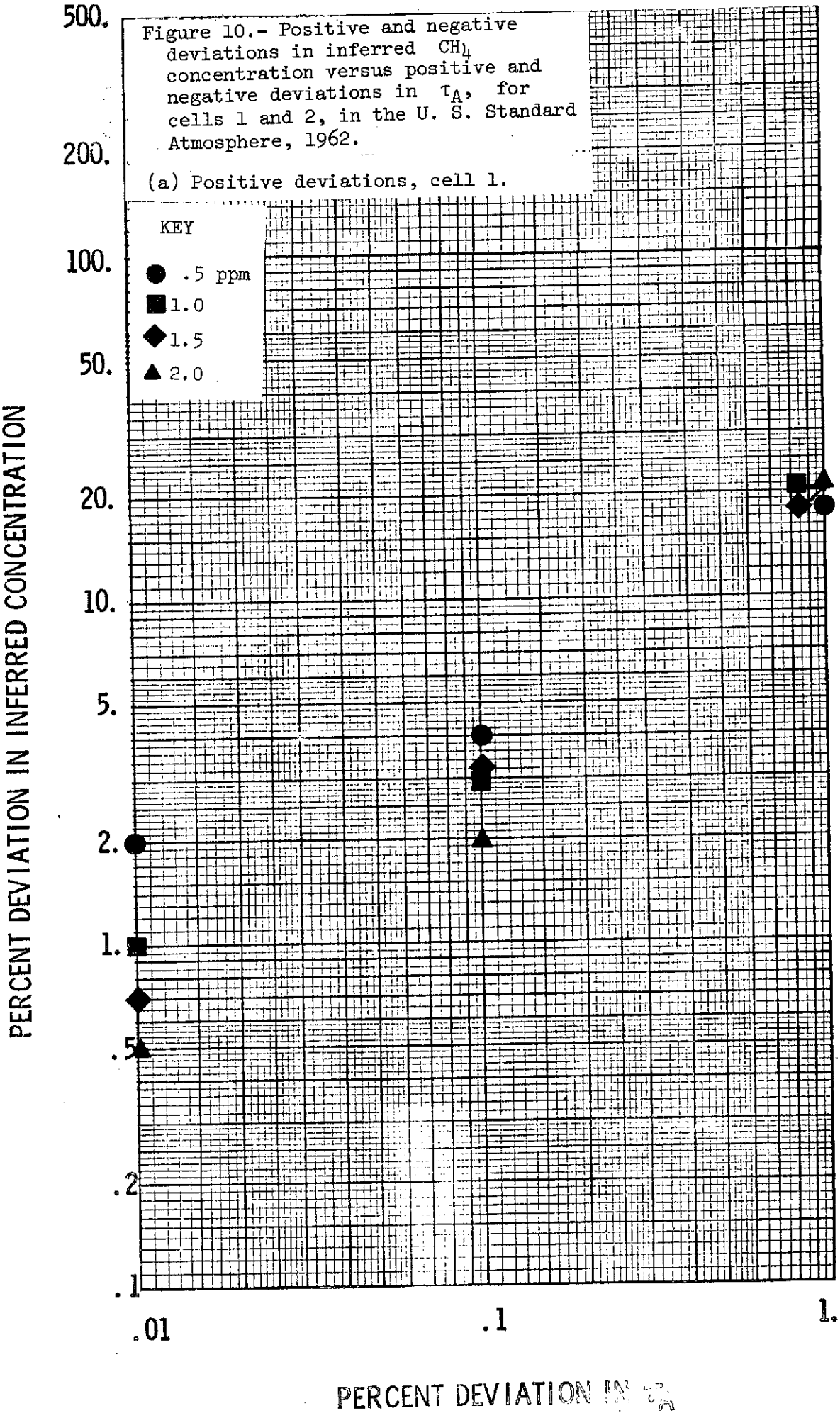

Figure 10.- Positive and negative deviations in inferred CH_4 concentration versus positive and negative deviations in τ_A, for cells 1 and 2, in the U. S. Standard Atmosphere, 1962.

(a) Positive deviations, cell 1.

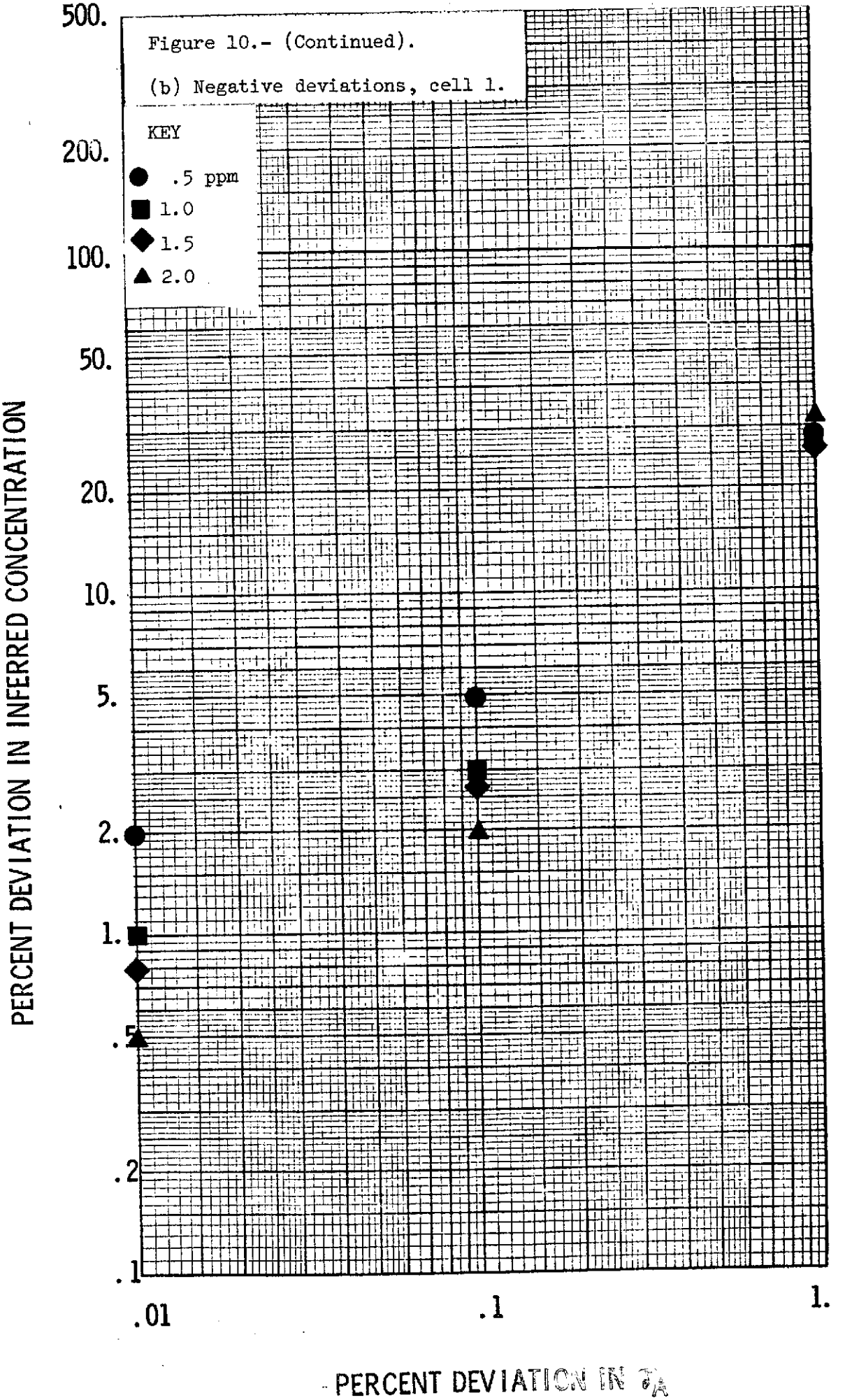
Figure 10.- (Continued).
(b) Negative deviations, cell 1.
KEY
.5 ppm
1.0
1.5
2.0
500.
200.
100.
50.
20.
10.
5.
2.
1.
.5
.2
.1
.01
.1
1.
PERCENT DEVIATION IN INFERRED CONCENTRATION
PERCENT DEVIATION IN

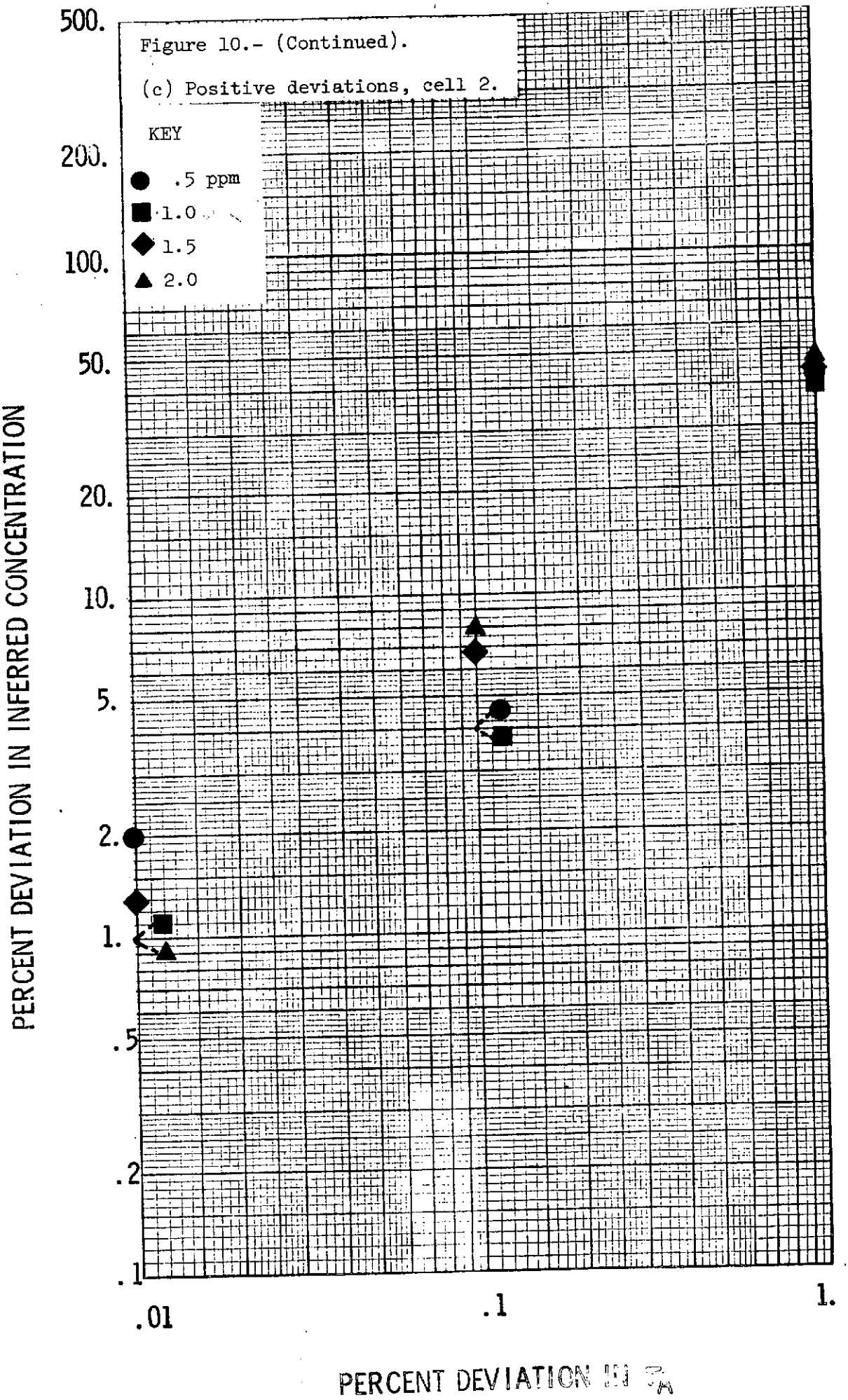
Figure 10.- (Continued).
(c) Positive deviations, cell 2.
KEY
.5 ppm
1.0
1.5
2.0
500.
200.
100.
50.
20.
10.
5.
2.
1.
.5
.2
.1
.01
.1
1.
PERCENT DEVIATION IN INFERRED CONCENTRATION
PERCENT DEVIATION IN

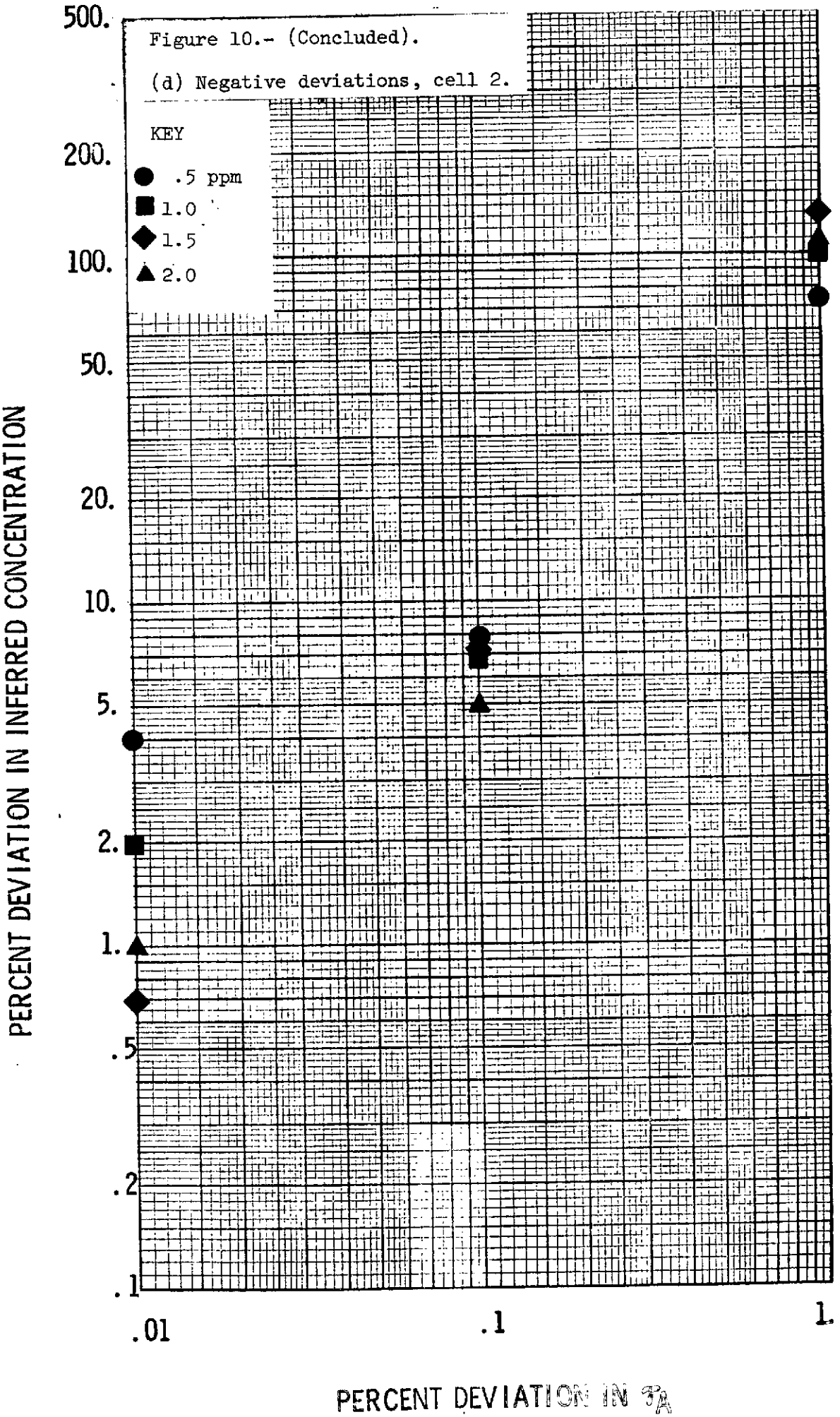
Figure 10.- (Concluded).
(d) Negative deviations, cell 2.
KEY
.5 ppm
1.0
1.5
2.0
500.
200.
100.
50.
20.
10.
5.
2.
1.
.5
.2
.1
.01
.1
1.
PERCENT DEVIATION IN INFERRED CONCENTRATION
PERCENT DEVIATION IN

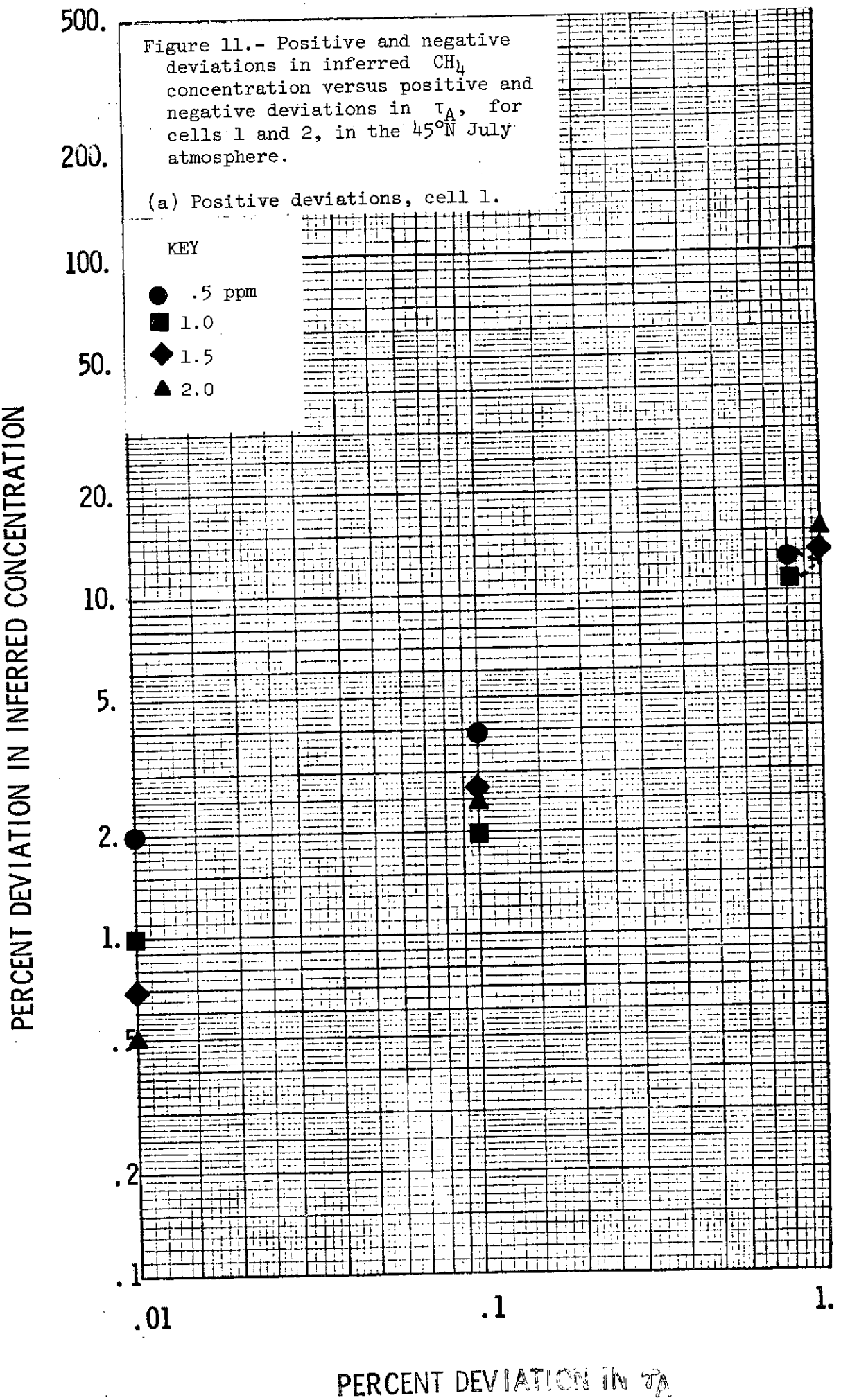
Figure 11.- Positive and negative deviations in inferred CH_4 concentration versus positive and negative deviations in τ_A, for cells 1 and 2, in the 45°N July atmosphere.
(a) Positive deviations, cell 1.
KEY
.5 ppm
1.0
1.5
2.0
500.
200.
100.
50.
20.
10.
5.
2.
1.
.5
.2
.1
.01
.1
1.
PERCENT DEVIATION IN INFERRED CONCENTRATION
PERCENT DEVIATION IN τ_A

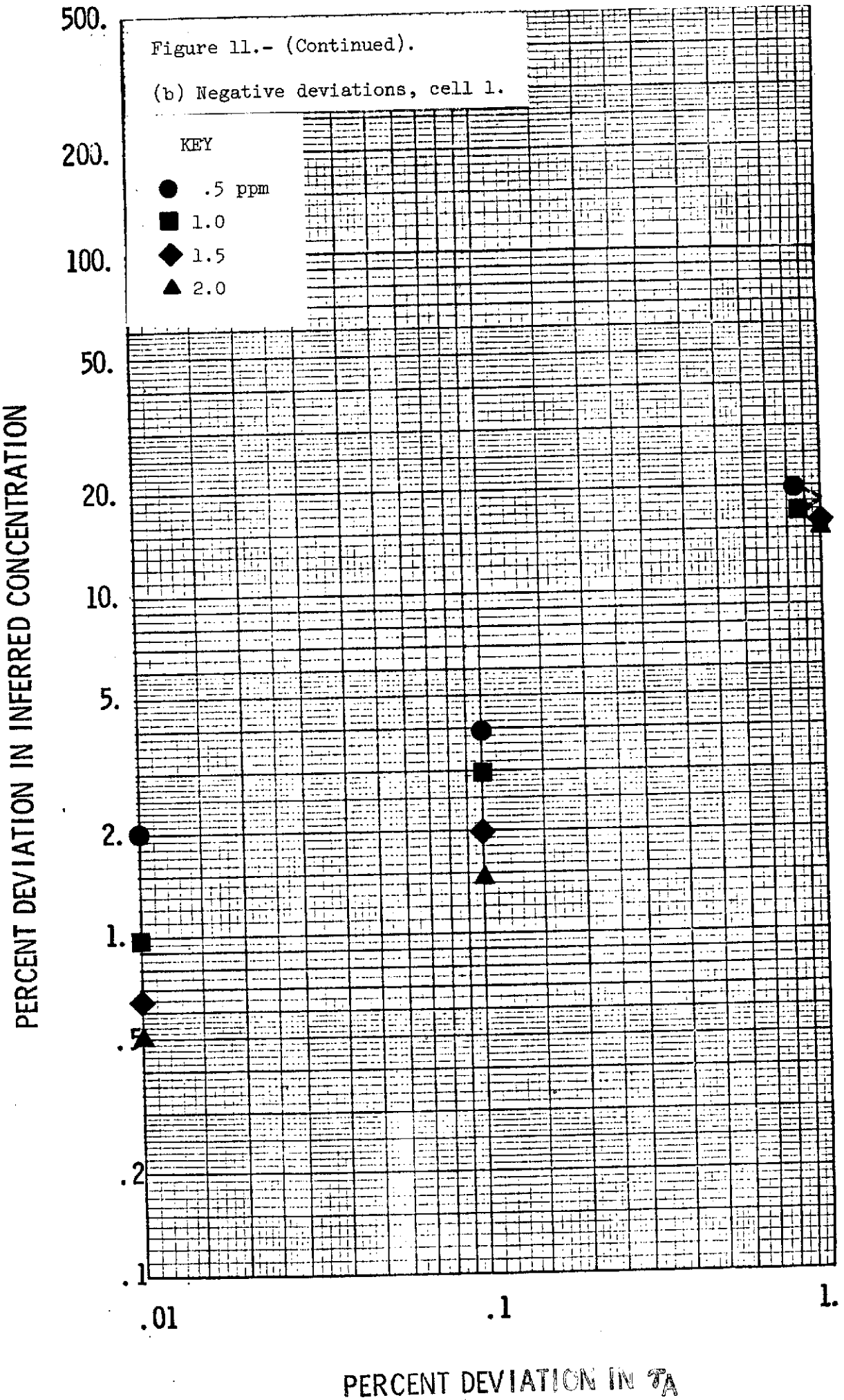
Figure 11.- (Continued).
(b) Negative deviations, cell 1.
KEY
.5 ppm
1.0
1.5
2.0
500.
200.
100.
50.
20.
10.
5.
2.
1.
.5
.2
.1
.01
.1
1.
PERCENT DEVIATION IN INFERRED CONCENTRATION
PERCENT DEVIATION IN T_A

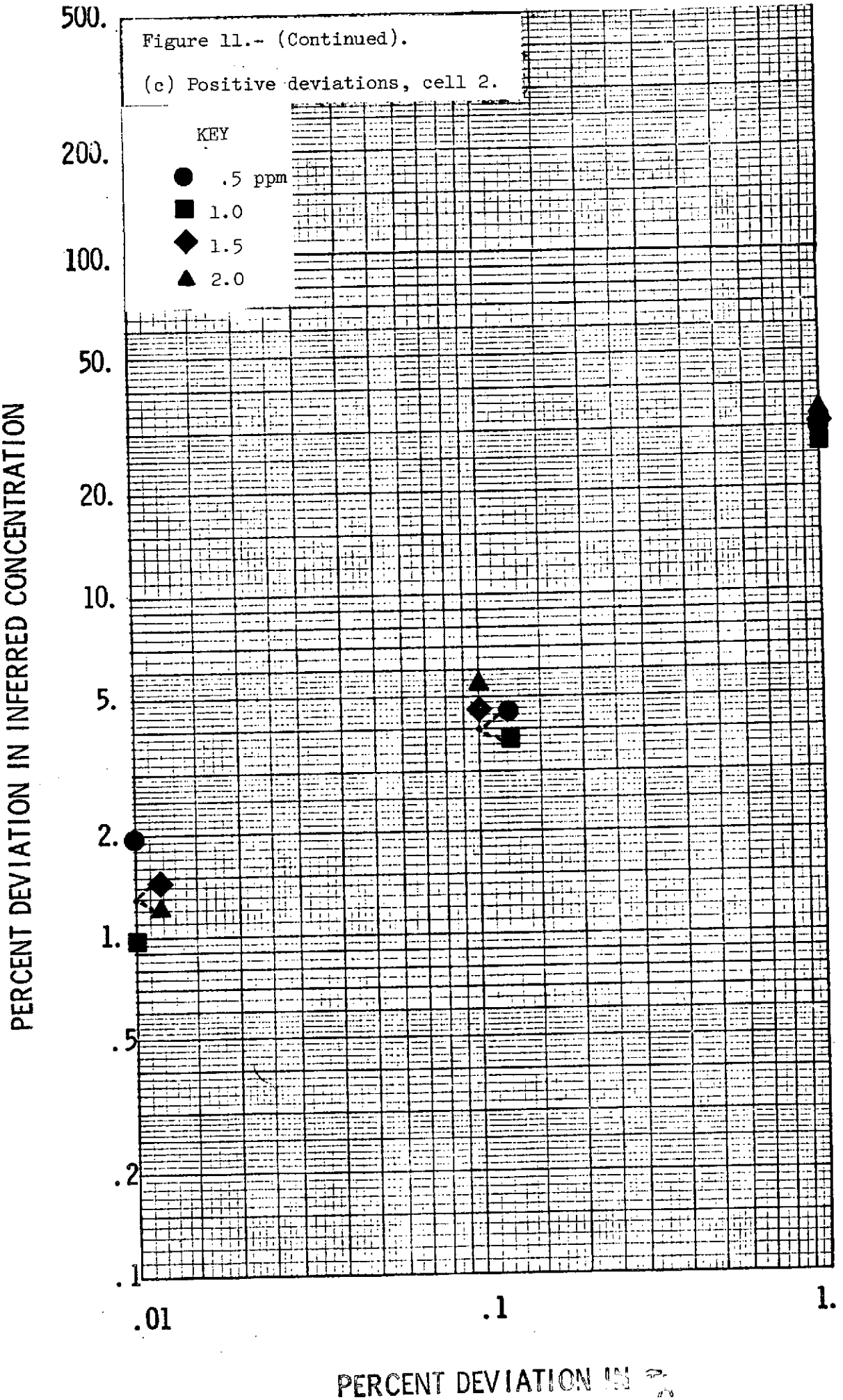
Figure 11.- (Continued).
(c) Positive deviations, cell 2.
KEY
.5 ppm
1.0
1.5
2.0
500.
200.
100.
50.
20.
10.
5.
2.
1.
.5
.2
.1
.01
.1
1.
PERCENT DEVIATION IN INFERRED CONCENTRATION
PERCENT DEVIATION IN

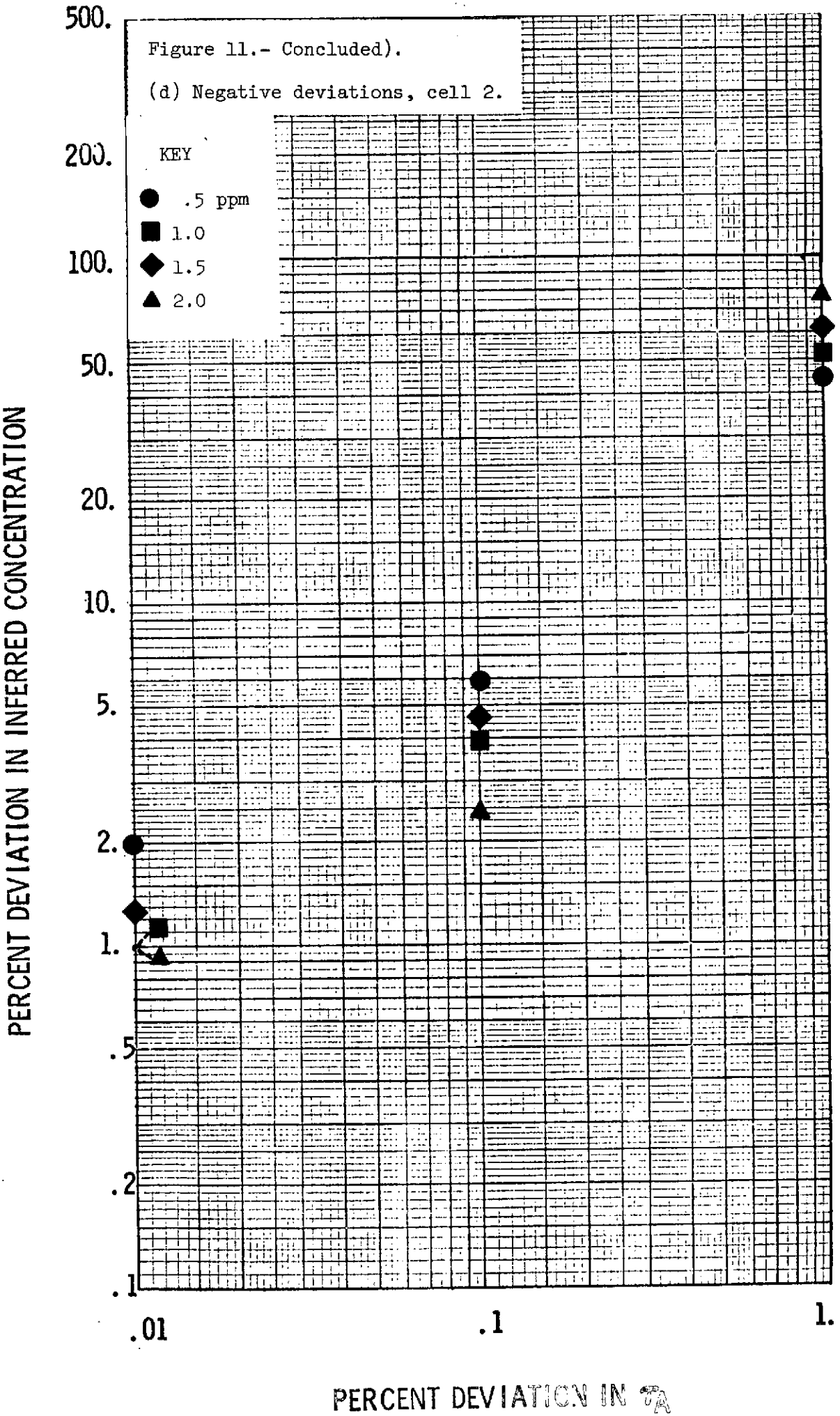
Figure 11.- Concluded).
(d) Negative deviations, cell 2.
KEY
.5 ppm
1.0
1.5
2.0
500.
200.
100.
50.
20.
10.
5.
2.
1.
.5
.2
.1
.01
.1
1.
PERCENT DEVIATION IN INFERRED CONCENTRATION
PERCENT DEVIATION IN

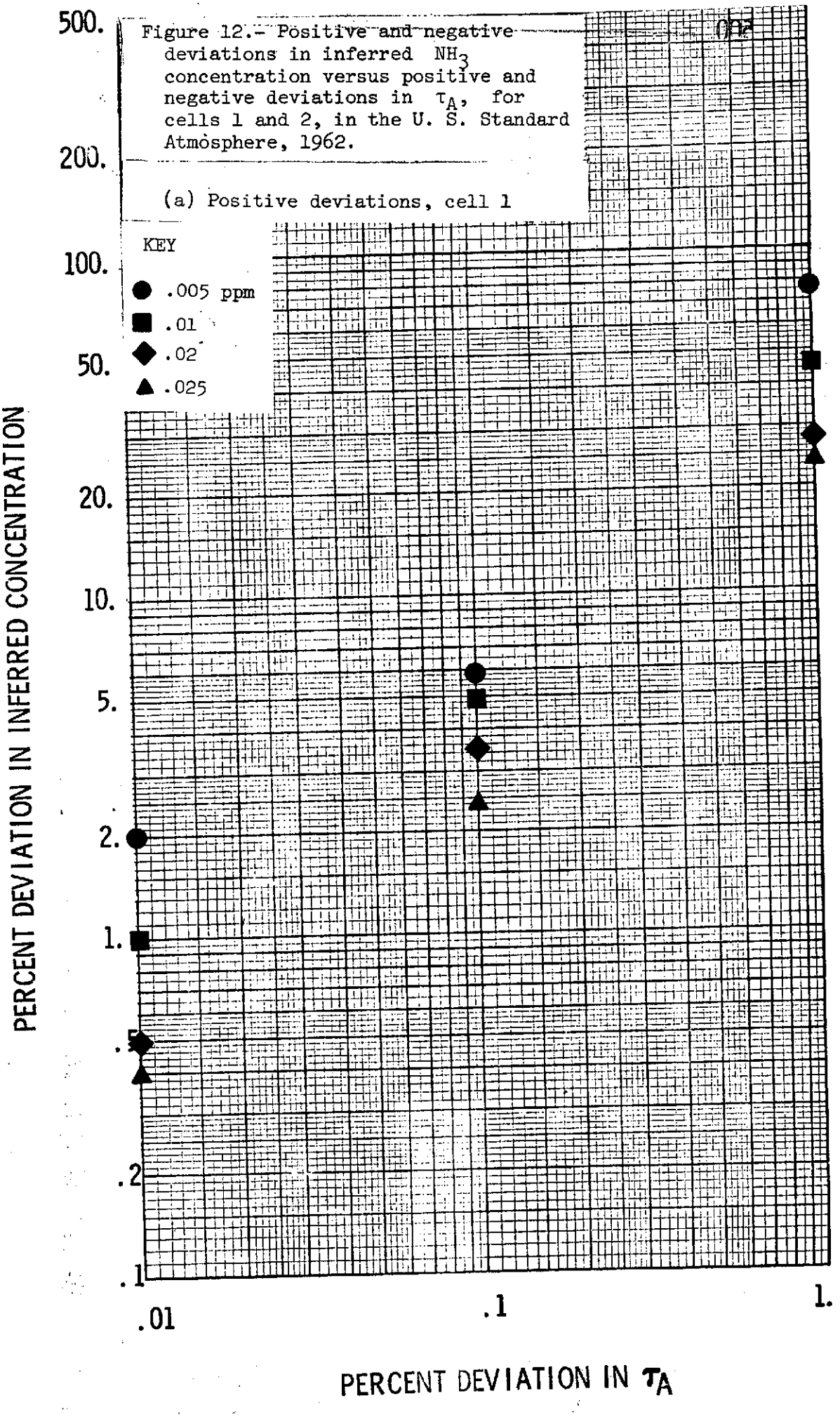
Figure 12.- Positive and negative deviations in inferred NH_3 concentration versus positive and negative deviations in τ_A, for cells 1 and 2, in the U. S. Standard Atmosphere, 1962.
(a) Positive deviations, cell 1
KEY
.005 ppm
.01
.02
.025
500.
200.
100.
50.
20.
10.
5.
2.
1.
.5
.2
.1
.01
.1
1.
PERCENT DEVIATION IN INFERRED CONCENTRATION
PERCENT DEVIATION IN τ_A

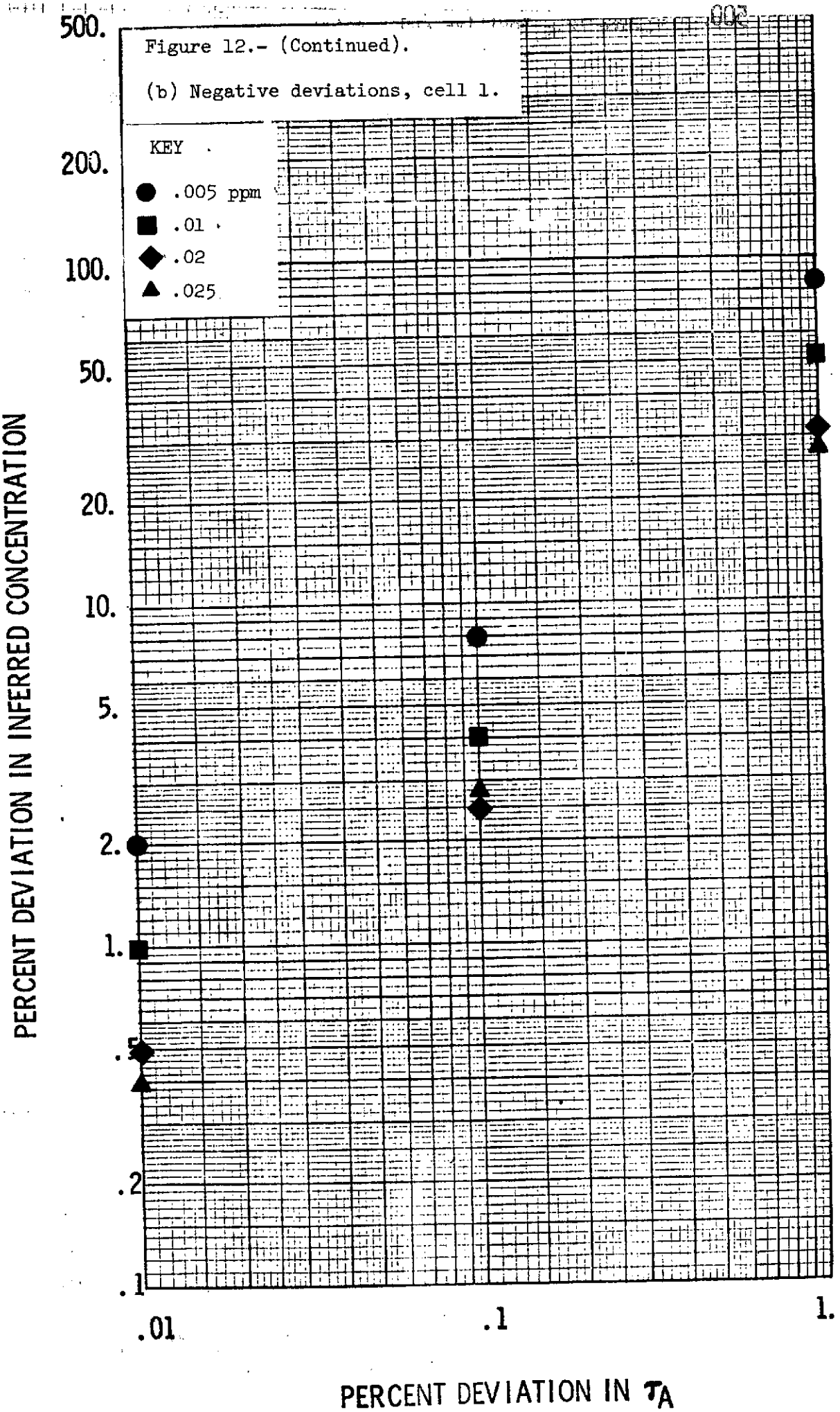
Figure 12.- (Continued).
(b) Negative deviations, cell 1.
KEY
.005 ppm
.01
.02
.025
500.
200.
100.
50.
20.
10.
5.
2.
1.
.5
.2
.1
.01
.1
1.
PERCENT DEVIATION IN INFERRED CONCENTRATION
PERCENT DEVIATION IN τ_A

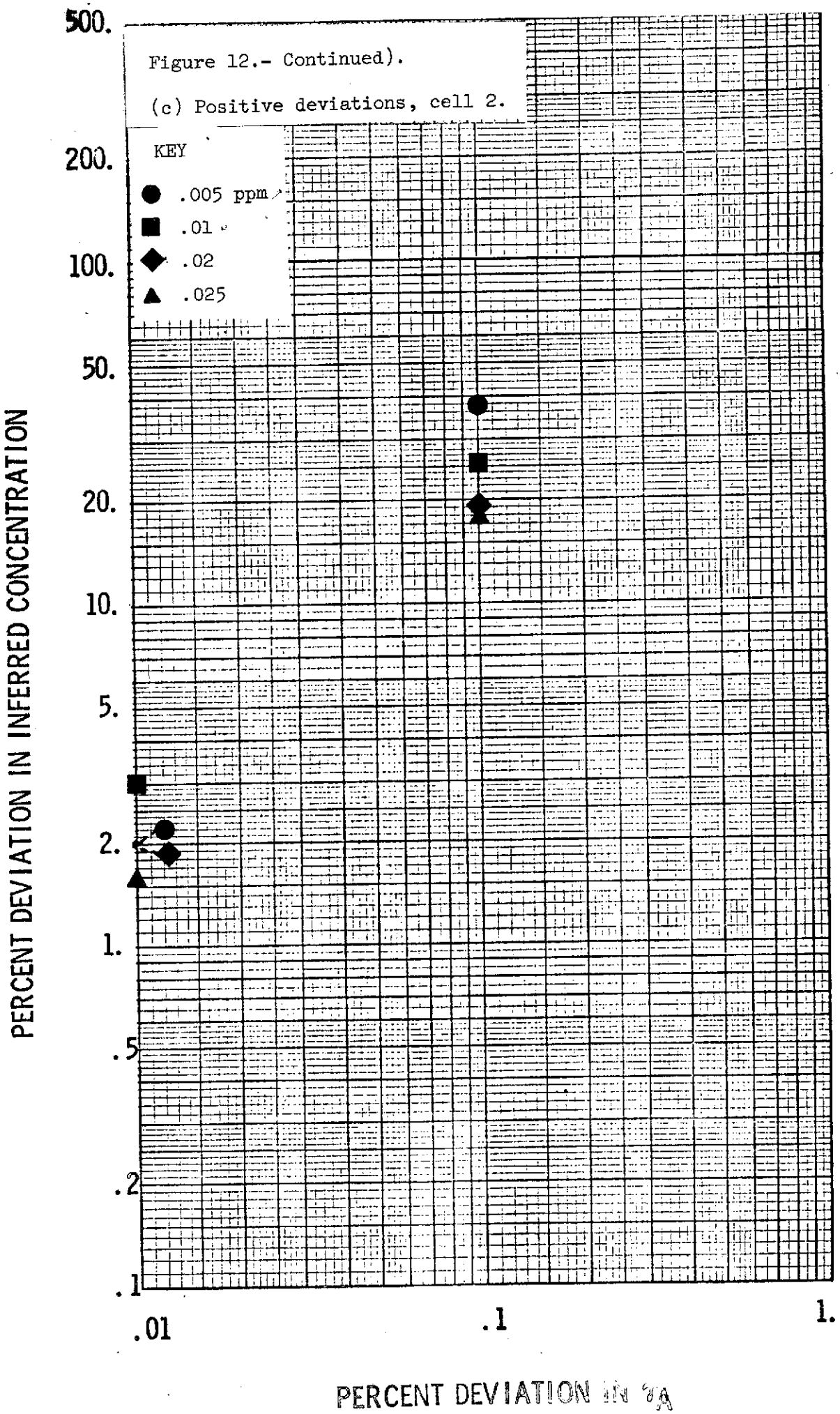
Figure 12.- Continued).
(c) Positive deviations, cell 2.
KEY
.005 ppm
.01
.02
.025
500.
200.
100.
50.
20.
10.
5.
2.
1.
.5
.2
.1
.01
.1
1.
PERCENT DEVIATION IN INFERRED CONCENTRATION
PERCENT DEVIATION IN

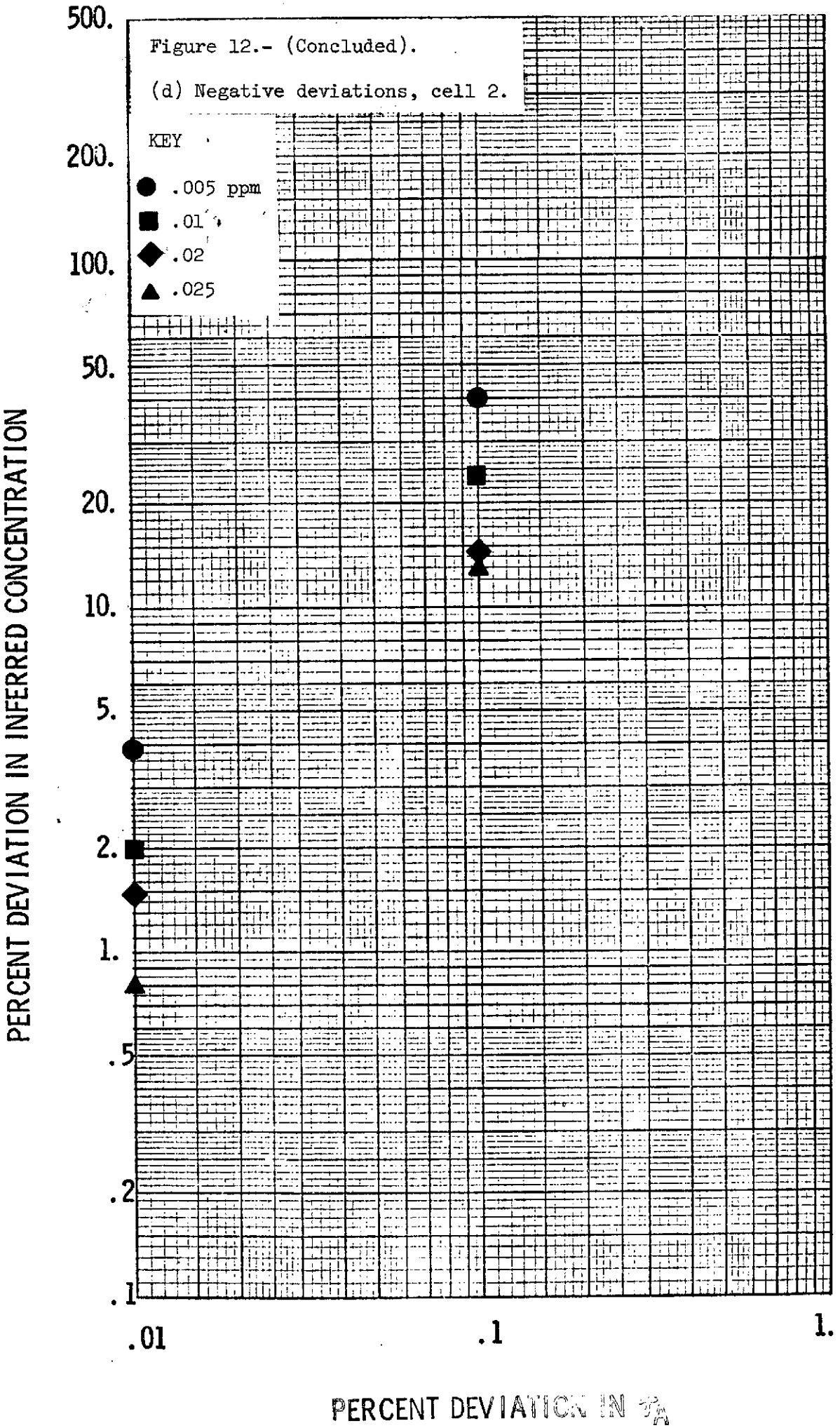
Figure 12.- (Concluded).
(d) Negative deviations, cell 2.
KEY
.005 ppm
.01
.02
.025
500.
200.
100.
50.
20.
10.
5.
2.
1.
.5
.2
.1
.01
.1
1.
PERCENT DEVIATION IN INFERRED CONCENTRATION
PERCENT DEVIATION IN

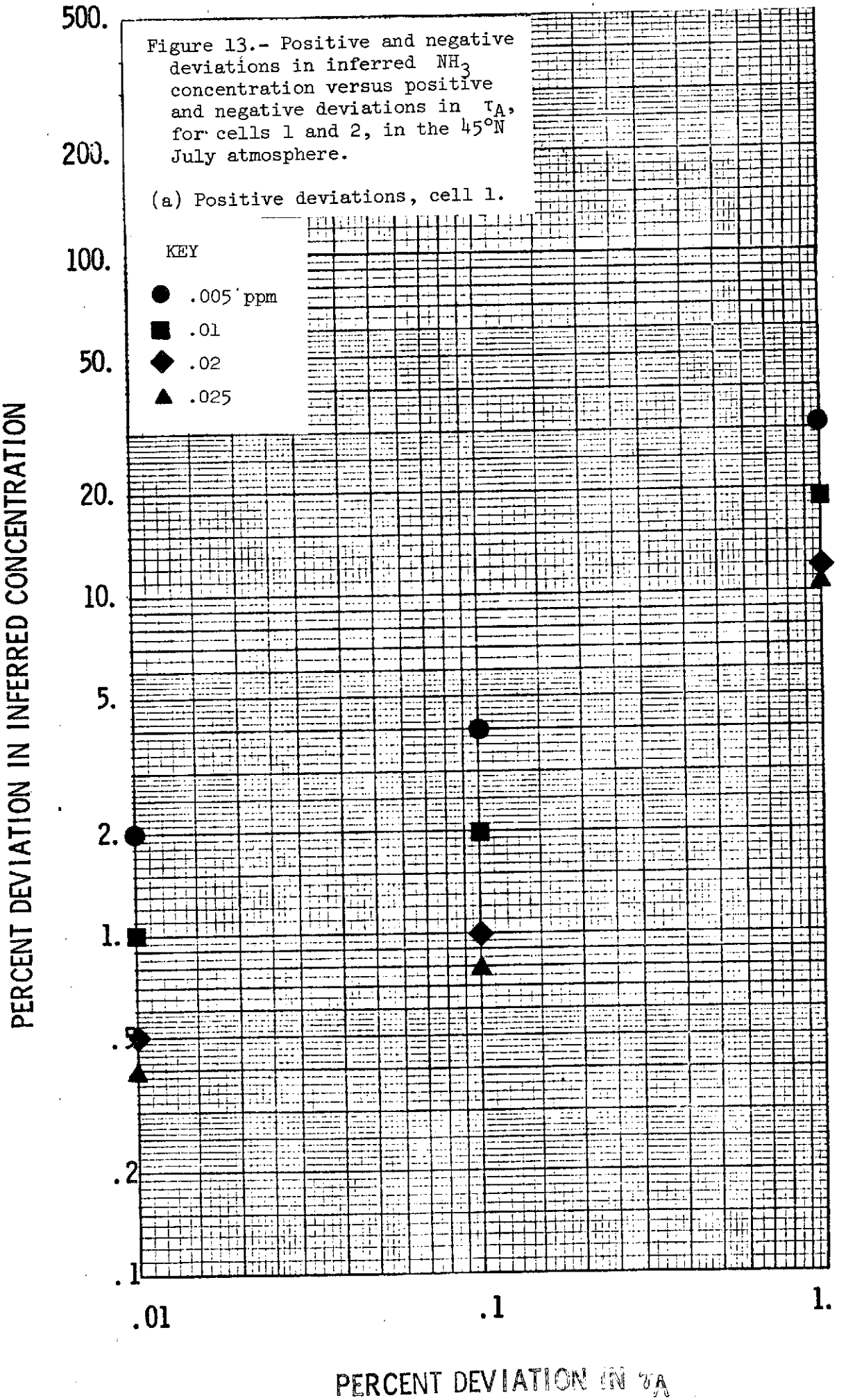

Figure 13.- Positive and negative deviations in inferred NH_3 concentration versus positive and negative deviations in τ_A, for cells 1 and 2, in the 45°N July atmosphere.

(a) Positive deviations, cell 1.

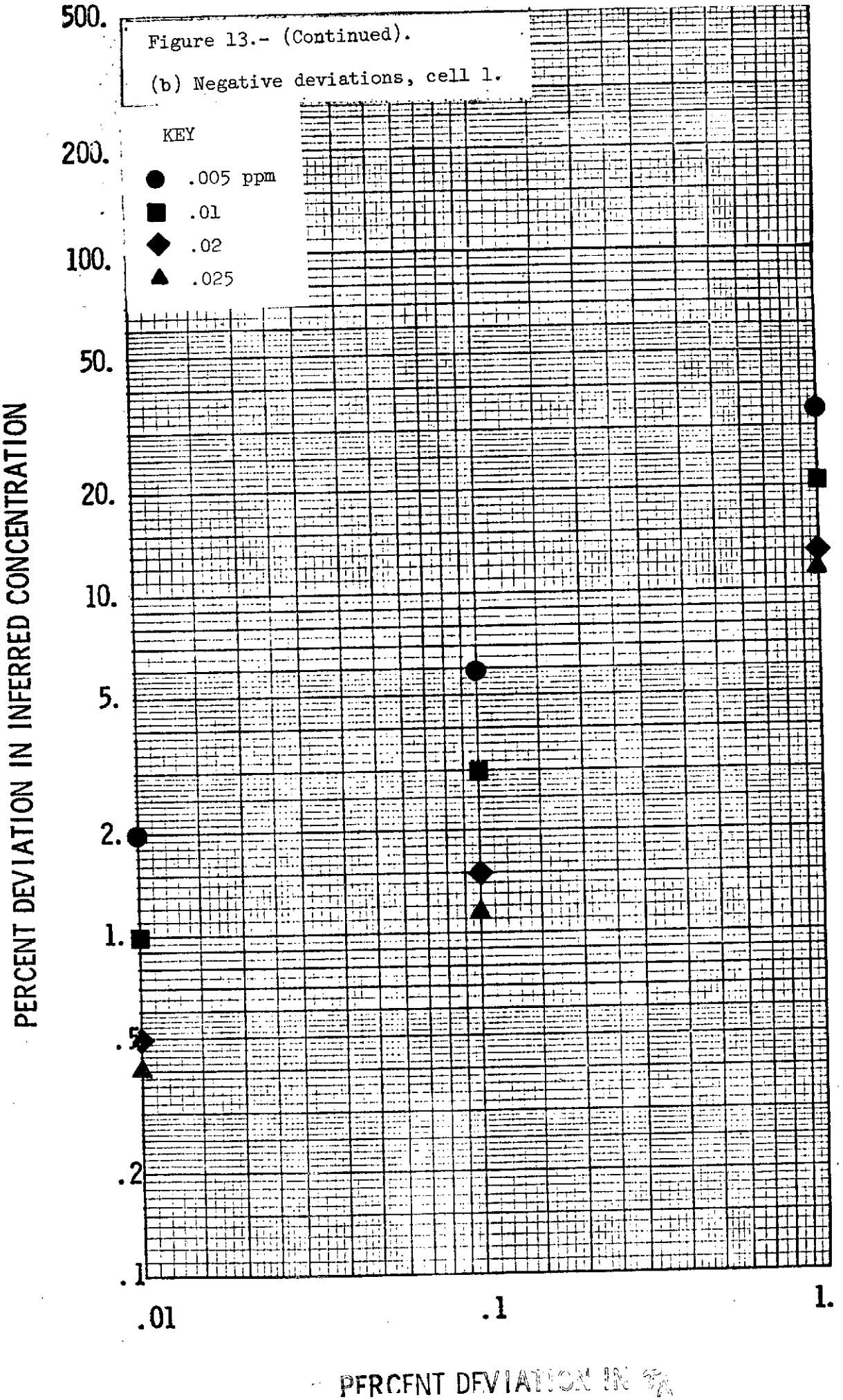

Figure 13.- (Continued).

(b) Negative deviations, cell 1.

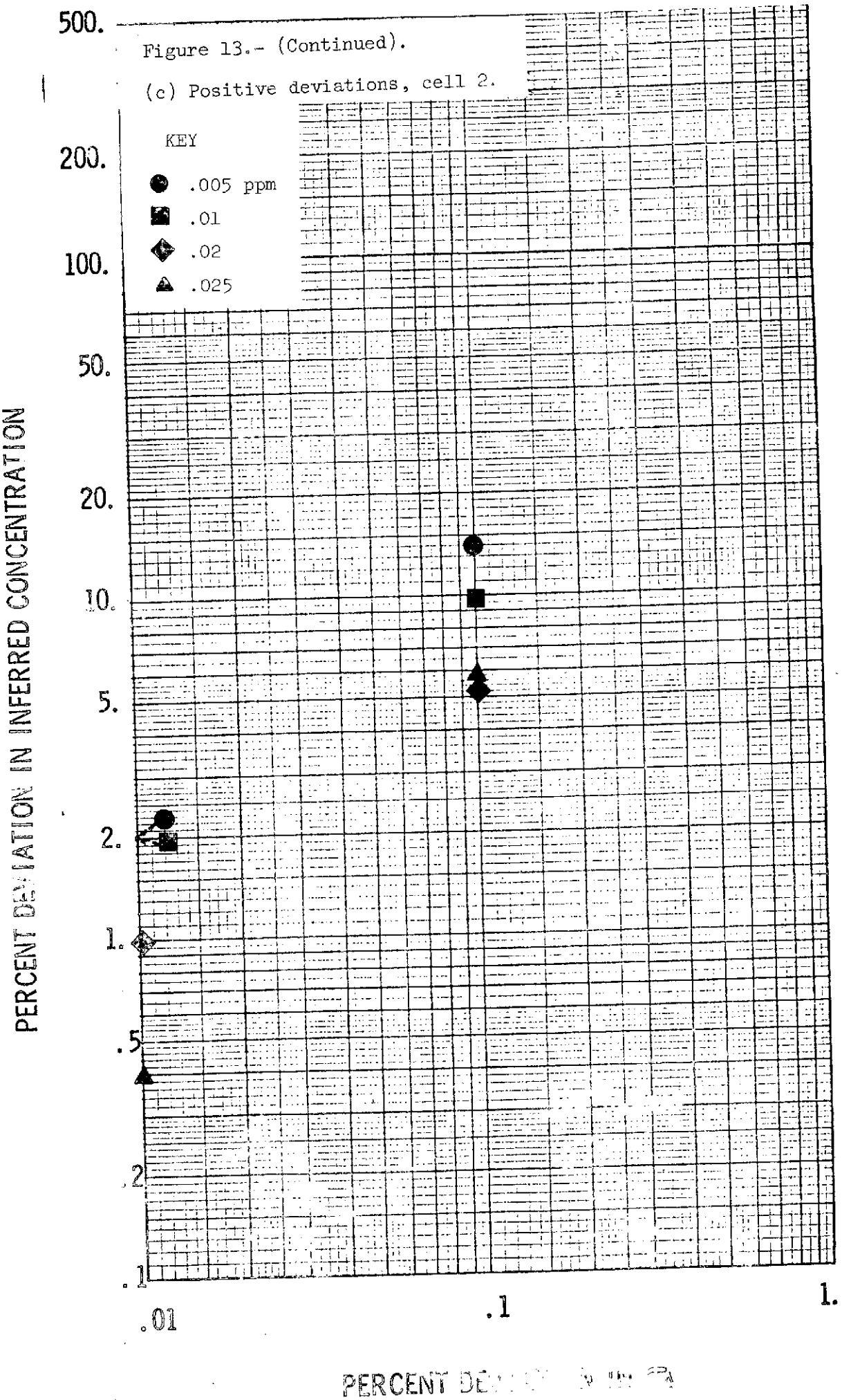
Figure 13.- (Continued).
(c) Positive deviations, cell 2.
KEY
.005 ppm
.01
.02
.025
500.
200.
100.
50.
20.
10.
5.
2.
1.
.5
.2
.1
.01
.1
1.
PERCENT DEVIATION IN INFERRED CONCENTRATION
PERCENT DE

Figure 13.- (Concluded).

(d) Negative deviations, cell 2.